Spring 2018

Fully differential study of dissociative capture in P + H_2 collisions

Basu Ram Lamichhane

Department: Physics

FULLY DIFFERENTIAL STUDY OF DISSOCIATIVE CAPTURE IN P + H_2 COLLISIONS

by

BASU RAM LAMICHHANE

A DISSERTATION

Presented to the Faculty of the Graduate School of the

MISSOURI UNIVERSITY OF SCIENCE AND TECHNOLOGY

In Partial Fulfillment of the Requirements for the Degree

DOCTOR OF PHILOSOPHY

in

PHYSICS

2018

Approved

Michael Schulz, Advisor
Don H. Madison
Yew San Hor
Daniel Fischer
Hyoung K. Lee

PUBLICATION DISSERTATION OPTION

This dissertation consists of the following two articles which have been published as follows:

Paper I: Pages 18-35 have been accepted by Physical Review Letters.

Paper II: Pages 36-63 have been accepted by Physical Review A.

ABSTRACT

In recent years, the key role of the projectile coherence properties has been studied in several ion-atom scattering processes. These studies strongly suggested that cross sections could be significantly affected by the projectile coherence properties, especially for fast, heavy ions. In the present study, we used such coherence effects as a tool to sensitively analyze the few- body dynamics of the scattering process. To this end, we performed three kinematically complete experiments on fragmentation of H_2 by 75 keV proton impacts. A novel approach was used to analyze coherence and interference effects in the observed cross-sections. The idea was to measure cross sections for coherent and incoherent projectiles simultaneously under otherwise identical experimental conditions. In the first experiment, single electron capture accompanied by vibrational dissociation was studied. Fully differential cross-sections (FDCS) were extracted for a fixed kinetic energy release and for two different fixed molecular orientations as a function of scattering angle. The coherent to incoherent FDCS ratios, which represents the interference term, revealed two distinct types of interference, single- and two-center interference. In the latter, an unexpected phase shift of π was found in the pronounced oscillations observed in the interference term. In the other two experiments, single capture accompanied by excitation of the second electron to a repulsive state, and Coulomb explosion due to double capture were studied. No clear signatures of single-center interference were observed for either process. Two-center interference was identified for dissociative transfer excitation. No π phase shift was observed for this process. Only a very weak two-center interference structure at most was found for double capture.

ACKNOWLEDGMENTS

First and foremost, I would like to express my sincere gratitude to my research advisor, Dr. Michael Schulz, for the continuous support, patience, and guidance towards my Ph.D. study and related research. His expertise and encouragement helped me to conduct my research smoothly. I consider myself very fortunate to work under his supervision. Besides my advisor, I would like to show gratitude to my committee: Dr. Don Madison, Dr. Yew San Hor, Dr. Daniel Fischer, and Dr. Hyoung K. Lee, for valuable discussions. I would like to thank Dr. Ahmad Hasan for assisting me with data analysis software and electronic equipments. It was an excellent learning experience with him.

I thank my friends and colleagues in the lab: Dr. Thusitha Arthnayaka, Dr. Sachin Sharma, Dr. Lomsadze, Madhav Dhital, Krishna Koirala, Sudip Gurung, Juan Remolina, and Trevor Voss, for the positive discussions, and for all the moments we have had in the last five years. Also, I would like to thank department chair, Dr. George D. Waddill, and academic advisor, Dr. Jerry L. Peacher; staff members Pamela J. Crabtree, Janice Gargus, Ronald Woody and Andrew L. Stubbs, for their help. I am also thankful to Dr. Bijay Shrestha, Nancy Uri, and Nepali friends of Rolla for making me feel at home.

I want to thank my mentor, Mr. Hari Saran Lamichhane, for his guidance and encouragement to choose science as a career.

Finally, my special thanks go to my parents, Shiva Kumar Lamichhane and Bhagawati Lamichhane, for their unconditional love and support. Also, I am thankful to my sister, Kamala, and all my relatives. Last but not the least, I would like to thank my wife, Asmita Phuyal, for her continuous love, support, and encouragement.

TABLE OF CONTENTS

SECTION

LIST OF ILLUSTRATIONS

SECTION

1. INTRODUCTION

The understanding of natural phenomenon requires addressing two fundamental questions. First, the forces acting between particles need to be understood. There are four fundamental forces in nature[1], namely the electromagnetic, weak, strong and gravitational forces, which are mediated by the exchange of other particles, the so-called gauge bosons. This mediation is basically a two-body process, as the gauge bosons can be emitted by only one particle and absorbed by one particle at a time. Among these forces, the electromagnetic force is essentially completely understood. Second, we need to know how systems consisting of more than two bodies develop under the influence of these pairwise acting forces. A satisfactory answer to the second question would unearth one of the most fundamentally important and yet unsolved problem in physics, known as the few-body problem (FBP). The essence of the FBP is that for a system consisting of more than two mutually interacting particles, the Schrödinger equation (or Dirac equation for relativistic cases) cannot be solved analytically even if the underlying forces are precisely known. Thus, theory has to resort to numerical modeling, and these models need to be tested by detailed experimental data.

With the advent of quantum mechanics, our knowledge of stationary systems on an atomic level had evolved extensively. Stationary systems are characterized by those states of a quantum system, which do not change with the evolution of time. For such systems

[1] Accounting for the unification of the electromagnetic and weak force, at most 3 fundamental forces are needed.

(e.g., stationary atoms) accurate information can often be obtained by using numerical methods, like for example, the multi-configuration Hartree-Fock approach [1]. However, for dynamic few body systems that evolve with time, the FBP represents a much bigger challenge.

Atomic collision experiments are particularly well suited to test the description of dynamic few-body systems because of two reasons [2-4]. First, the underlying fundamental interaction in atomic systems, the electromagnetic force, is essentially completely understood. In contrast, for nuclear systems, the underlying nuclear force is not nearly as well understood as the electromagnetic force. Therefore, it is not clear whether experiments are testing the theoretical descriptions of the underlying forces or of the few body dynamics. Second, atomic collision experiments investigate systems consisting of small particle numbers, for which the complete kinematics of each particle involved in the system can be determined experimentally (kinematically complete experiments). In contrast, solid-state systems typically deal with particle numbers of the order of Avogadro's number (N_A). Obviously, for such large particle numbers, it is not possible to perform kinematically complete experiments. For such systems only statistically averaged or collective quantities can be measured, which do not provide a sensitive test of the theoretical description of the reaction dynamics. Hence, a potential lack of understanding of the few body dynamics could simply be hidden in the statistics over a huge particle number.

Kinematically complete experiments, in which the complete momentum vectors of all the collision fragments are measured, are critical to advance our understanding of the FBP as they offer the most sensitive tests of theory. For electron impact ionization excellent agreement between theory and such experiments for simple one- or two- electron targets

are now routinely achieved [5-7]. On the other hand, the few body dynamics for ion impact collisions is not nearly as well understood. Ion impact experiments are much more challenging because of the larger projectile mass compared to electrons. This leads to very small (for fast, heavy ions immeasurably small) scattering angles and energy losses relative to the initial projectile energy. From a theoretical point of view, one major challenge is that a very large number of angular momentum states contribute to the scattered projectile state. The experimental problems were overcome with the development of cold target recoil-ion momentum spectroscopy (COLTRIMS). Kinematically complete experiments then became feasible by directly measuring the momenta of the recoil ions and of the ejected electrons or, for light ions at small and intermediate speeds, of the recoil ions and of the scattered projectiles [8-11].

In atomic fragmentation experiments, a useful parameter to characterize the nature of the collision is the perturbation parameter (η), i.e., the projectile charge to speed ratio. Experimental data were reproduced well by various calculations based on perturbative and non-perturbative models for a system with small η in the scattering plane, which is spanned by the initial projectile momentum vector and the momentum transfer vector. Even a rather simple first-born approximation (FBA) model is usually able to reproduce the experimental data for electron and ion impact collisions with small η [12-14]. Therefore, it was believed that the collision dynamics in this kinematic region is to a large extent understood even in the case of ion impact. However, even very sophisticated higher-order theoretical models [15-17] failed to reproduce the experimental data [18-20] of measured FDCS for ion impact outside the scattering plane.

Schulz et al. [2] measured the fully differential cross sections (FDCS) for single ionization of He by 100 MeV/a.m.u. C^{6+} ions. The measured fully differential three-dimensional angular distribution of the ejected electrons is plotted in Figure 1.1(a). The direction of the initial projectile beam is labeled as $\mathbf{p}_0$, and the momentum transfer from the projectile to target is given by **q**. A clear peak structure was observed in the direction of the momentum transfer (**q**), the so-called binary peak. Also, another structure, but with a smaller peak intensity, was observed in the direction opposite to **q**, the so-called recoil peak.

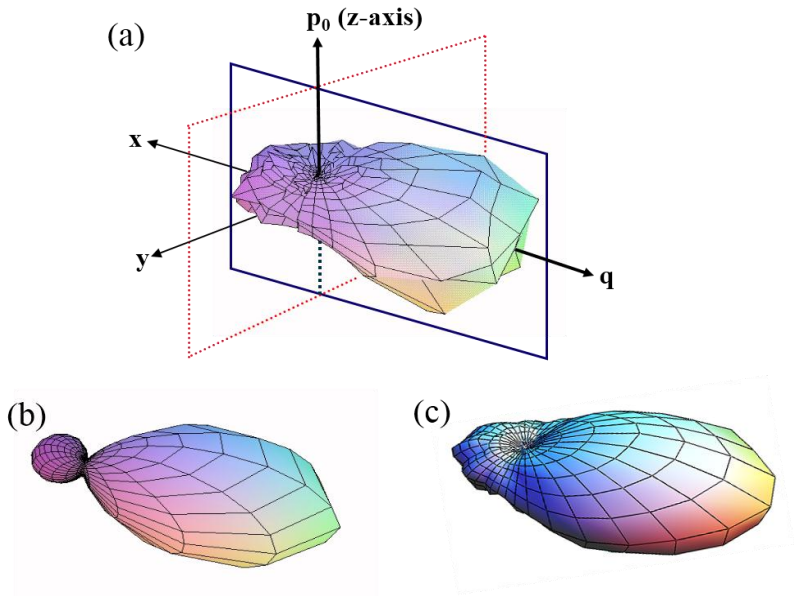

Figure 1.1. Three-dimensional angular distribution of ejected electron momenta for ionization of He by 100MeV/a.m.u. C^{6+}. (a) Experiment (b) 3DW calculations (c) FBA convoluted with classical elastic scattering.

Very surprising discrepancies between experimental data and fully quantum mechanical (QM) calculations were found. As an example, Figure 1.1(b) shows a very sophisticated state of the art calculation, based on the three-body distorted wave (3DW)

approximation [21]. The experimental data were well reproduced in the scattering plane (blue color plane) in Figure 1.1(a). However, the agreement is very poor outside the scattering plane. The 3DW calculation predicts a pronounced double peak structure separated by a distinct minimum at the origin, however, this minimum is almost completely filled up in the experimental result. Even more surprisingly, a less sophisticated model shown in Figure 1.1(c), which treats the projectile-target nucleus scattering classically, yielded a much-improved agreement as it reproduces the filling of the minimum at the origin between the binary and recoil peak structures. Here, the calculation was based on the FBA, which was convoluted with classical elastic scattering between the projectile and the target nucleus [22].

All fully QM calculations reported so far are basically afflicted with the same discrepancies to experiment. This provokes the question whether all of these models share the same fundamental problem as the 3DW model [16,21,23,24], which for some reason does not affect (semi-)classical treatments like the convolution of the FBA with classical elastic scattering. One property, which all QM models, but not the (semi-) classical treatments, have in common, is that they all describe the projectiles by delocalized waves, i.e., as an entirely coherent beam. In other terms, the width of the projectile wave packet is much larger than the dimension of the target. For electron impact experiments this is a reasonable assumption as the coherence length is almost always much larger than the target dimension because of the much larger de Broglie wavelengths of electrons compared to ions. Thus, the approximation of treating the projectile as a fully coherent wave turns out to be realistic. However, the commonly applied notion of the projectile to be completely delocalized might not always be valid for fast and heavy ions. Because of the large inherent

momentum uncertainty for fast and heavy ion impact, the projectiles tend to be more localized.

The measured cross section could sensitively depend on the projectile coherence properties. Interference effects predicted by theory might not be observable in experiments because of a lack of coherence, which could explain the discrepancies, described above. One possibility to test the role of coherence experimentally is to study processes for which cross- sections are known to exhibit interference structures in the case of a coherent beam. Young double-slit type or molecular two-center interference was observed in differential cross sections for various processes in collisions with molecular targets [25-31]. It is due to indistinguishable scattering from the two (or more) atomic centers of the molecule. One cannot distinguish from which center the scattered projectile wave is diffracted; thus, all contributions must be added coherently, which leads to the observable interference structure. However, one requirement for such interference to be observable is that the projectile beam needs to be coherent. In other words, to observe interference the width of the projectile wave packet, or its transverse coherence length (Δx), must be large enough to coherently illuminate both scattering centers simultaneously.

The coherence length can be controlled experimentally to some extent by placing collimating slits at a variable distance from the target before the collision region. In analogy to classical optics, the following relation gives the transverse coherence length; Δx:

$$\Delta x = \lambda \left(\frac{L}{2a}\right) \qquad (1)$$

where L is the distance of the slit to the target, a is the width of the collimating slit, and λ is the de-Broglie wavelength of the projectiles. Depending on the transverse coherence

length of the projectile compared to the dimension of the diffracting object (**D**), a projectile beam can be considered localized or delocalized, in other words, coherent or incoherent respectively as shown in Figure 1.2.

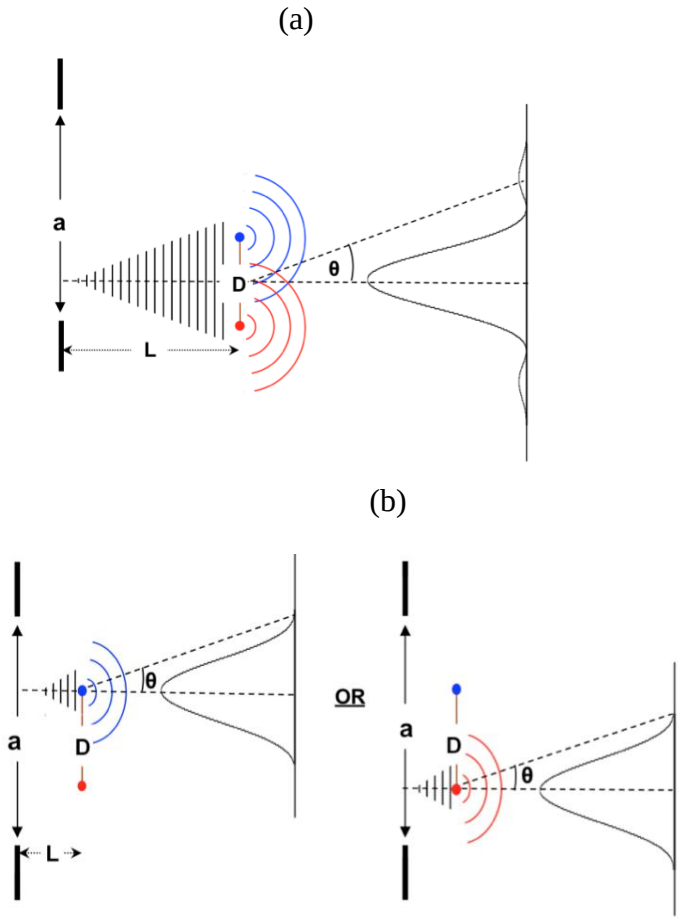

Figure 1.2. Illustration of visibility of molecular two-center interference (a)large L means $\Delta x >$ **D** and interference should be present (b) small L means $\Delta x <$ **D** and interference should be absent.

If the collimating slit is far away from the target such that Δx is larger than **D** (Figure 1.2 a), the same projectile wave packet can simultaneously illuminate both scattering centers. In this case, the diffracted waves from the two atomic centers should be added coherently; an interference pattern is present. On the other hand, if L is small (Figure

1.2 b), so that Δx is smaller than **D** only one atom will be illuminated at a time, and no interference structure will be present.

Since molecular two-center interference was studied as the first test of potential coherence effects, in the following a brief review is given. It was first predicted in 1960 by Tuan and Gerjuoy [32] for a charge transfer process and later also by Cohen and Fano [33] for photoionization. It was experimentally confirmed about 30 years later when the angular distribution of the fragments produced in dissociation of deuterium by electron capture and ionization by bare oxygen ion impact was measured [25]. It was observed that deuterium molecules are more likely to be aligned perpendicular to the incident beam than parallel to the beam. This feature was interpreted as due to an interference of capture amplitudes from the two atomic centers. Interference patterns have been reported in further studies of ion impact ionization of H_2 [26-31,34]. However, in many cases, the observed structures were weak and became evident only after normalizing to theoretical ionization cross sections for atomic hydrogen.

In analogy to classical optics, the interference term(IT) can be expressed as a ratio R between the cross sections for the coherent and incoherent beam:

$$IT = R = \frac{Coherent\ cross{-}section}{Incoherent\ cross{-}section} \qquad (2)$$

Theoretically, the interference term for molecular two-center interference for fixed molecular orientation is given by [26,35]

$$IT = 1 + \cos(\boldsymbol{P}_{rec} . \boldsymbol{D}) \qquad (3)$$

Here, the dot product between the recoil-ion momentum ($\mathbf{P}_{rec}$) and the inter-nuclear separation vector (**D**) of the molecule is the phase angle (δ) of the interference term.

Recently, two-center interference was reported in measured cross-sections for dissociative capture [30] and excitation [36] with simultaneous target ionization in collisions between H^{2+} molecular ions and helium atoms. In both experiments, an unexpected double slit interference pattern was observed. When this pattern was compared to the optical double slit, interference minima and maxima were found interchanged. This observation was explained by the switch in symmetry in the electronic part of the wave function. This explanation is an application of parity conservation. To conserve the total parity of the system, the projectile must switch its symmetry to compensate the switch in the symmetry of the electronic state, and this should lead to a π phase shift in the interference term. The experimental data were well reproduced by the interference term:

$$IT = 1 + \cos(\boldsymbol{P}_{rec} . \boldsymbol{D} + \pi) \quad (4)$$

In the research outlined in this thesis, a similar phase shift in the interference term was observed in vibrational dissociation of molecular hydrogen by proton impact, although, no switch in the electronic part of the wave function was involved in the transition. The results of this experiment will be discussed in the first part of this thesis in journal Paper I.

Two-center interference was used by Egodapitiya et al. [31] to study the effect of projectile coherence properties in ionization of molecular hydrogen by 75keV proton impact. Two different coherence lengths were used in the experiment by varying the slit distance to the target. A large slit distance was set to provide $\Delta x \approx 3.3$ a.u., whereas a smaller slit distance corresponded to $\Delta x \approx 1$ a.u. As the separation of the two atomic centers, **D** for the hydrogen molecule is 1.4 a.u., a coherent and incoherent beam was created by the large and small slit distance respectively. In that work, significant

differences were observed in the scattering angle dependence of double differential cross sections(DDCS) between the coherent and incoherent projectile beam. An interference structure was found only for a coherent projectile beam, but it was absent for an incoherent beam. The interpretation of these differences as being caused by coherence effects did not go completely unchallenged. For example, Feagin and Hargreaves argued that they are merely due to beam divergence effects [37]. However; this assertion was refuted by Sharma et al. [38], who experimentally demonstrated that the beam divergence was not large enough to explain the differences observed for the large and small slit distances.

Furthermore, the presence of such coherence effects was confirmed by a series of subsequent fully differential studies on similar collision systems [39-41] as well as by theoretical investigations [42-44]. Sharma et al. [39] performed a kinematically complete experiment for single ionization of H_2 by 75keV proton impact for a fixed projectile energy loss of 30 eV. They measured and analyzed FDCS for the projectile beam with varied coherence lengths. Here, too, significant and qualitative differences in measured cross sections were observed depending on the transverse coherence length (Δx) of the projectile beam. Signatures of two distinct types of interference were seen, namely single- and two-center interference, by varying different kinematics parameters; however, the FDCS were not sensitive enough to clearly distinguish between these two kinds of interference. For the latter, they initially explained interference as due to first- and higher order ionization amplitudes interfering with each other. They observed that the momentum transfer rather than the recoil-ion momentum primarily determined the phase angle in the interference term and a simple model single-center interference term was suggested as,

$$IT = 1 + \alpha \cos\left(q_{tr}\, \Delta b\right) \tag{5}$$

Here, α accounts for damping of the interference due to incomplete coherence, and due to experimental resolution, Δb represents an effective impact parameter range, and q_{tr} is transverse momentum transfer.

However, it was previously believed that the recoil-ion momentum determined the phase angle in molecular two-center interference. The results of [39] indicated that either single center interference dominated over two- center interference or the previous assumption that the recoil-ion momentum primarily defines the phase angle in molecular two-center interference was incorrect. To address this question, Arthanayaka et al. [40] studied fully differential cross sections for single ionization of H_2 by 75keV proton impact with the same collimating slit settings but for a higher projectile energy loss of 57eV. The aim was to more clearly distinguish between single- and two-center interference and to investigate the nature of the former type of interference.

In that work, the FDCS for coherent and incoherent projectile beam were analyzed as a function of the azimuthal electron emission angle (ϕ_{el}) for fixed polar electron emission angle (θ_{el}) and either fixed momentum transfer (**q**) or fixed recoil momentum ($\mathbf{P}_{rec}$). In the case of fixed **q**, ϕ_{el} unambiguously determines the recoil-ion momentum, and in case of fixed $\mathbf{P}_{rec,}$ ϕ_{el} determines **q**. In the ratio R of coherent to incoherent FDCS for fixed **q**, a pronounced interference structure was observed as shown in Figure 1.3(a). This structure was interpreted as a molecular two-center interference, where the recoil-ion momentum yields the phase angle. However, the observation that the interference pattern depends on $\mathbf{P}_{rec}$ does not necessarily mean that single-center interference does not play any role. To study potential contribution from the single-center interference, data were also analyzed for fixed recoil-ion momentum, i.e., as a function of q. A pronounced interference structure

was observed as shown in Figure 1.3 (b), which was interpreted as the single-center interference suggested by Sharma et al. [39]. This experiment demonstrated the importance of both single and two-center interference in ionization of H_2 and fixing either the momentum transfer or the recoil momentum of the FDCS, respectively, separated both types of interference structures.

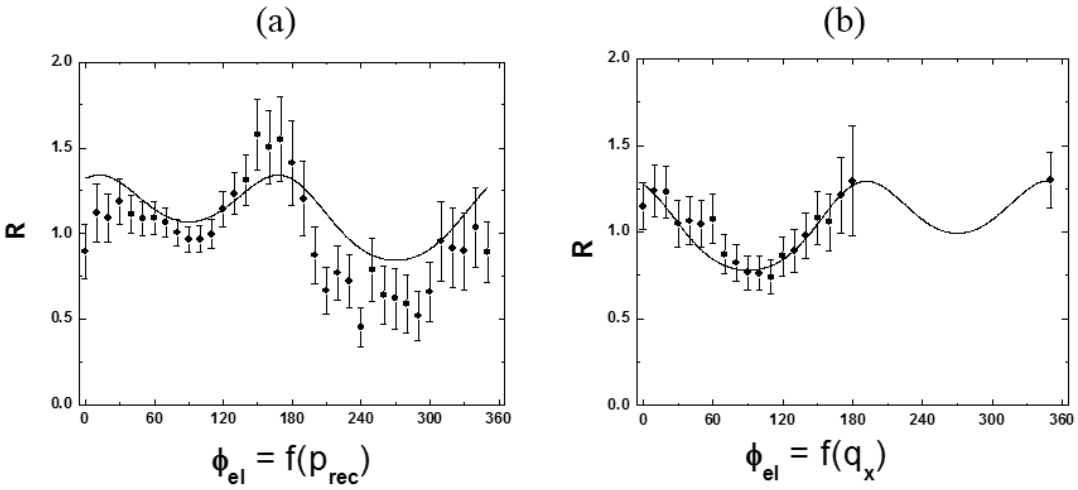

Figure 1.3. Fully differential cross section ratios between the large and small slit distance as a function of azimuthal electron emission angle for (a) fixed transverse component of momentum transfer at 1.4 a.u. and (b) for fixed recoil-ion momentum at 0.2 a.u. The polar angle was fixed at 35°. The solid curves were obtained (a) from $IT = 1 + \alpha cos\ (\boldsymbol{P}_{rec}.\ \boldsymbol{D})$ for D = 1.4 a.u. and $\alpha = 0.5$, and (b) from $IT = 1 + \alpha\ cos\ (q_{tr}\ \Delta b)$ for $\Delta b = 2$ a.u. and $\alpha = 0.3$.

Although the above-mentioned experiments have significantly advanced our understanding of coherence and interference effects, its analysis is nevertheless challenging because of the simultaneous existence of both types of interference for molecular targets. To address this problem, Arthanayaka et al. [41] studied fully differential cross sections for an atomic helium target with the same projectile beam and collimating slit settings for a projectile energy loss of 30eV. The motivation was to unambiguously identify single-

center interference because of the selection of the atomic target. To study coherence and the interference term in detail, fully differential cross-sectional ratios R were analyzed (Figure 1.4) for fixed recoil-ion momentum as a function of the azimuthal electron emission angle (ϕ_{el}). The structures observed in R were consistent with the single-center interference term given by Eq. (5).

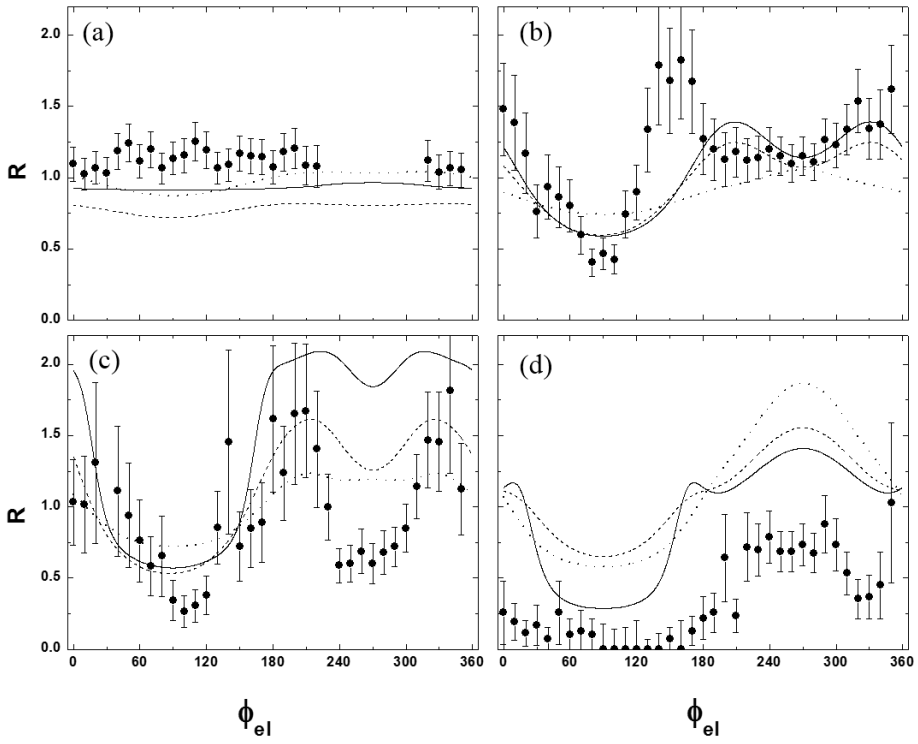

Figure 1.4. Ratios between FDCS for coherent and incoherent beams for p_{recx} = 0.2 a.u. and θ_{el} = 25° (panel (a)), p_{recx} = 0.7 a.u. and θ_{el} = 45° (panel (b)), p_{recx} = 0.7 a.u. and θ_{el} = 65° (panel (c)), and p_{recx} = 1.25 a.u. and θ_{el} = 65° (panel (d)) as a function φ_{el}. Dotted curves: first order treatment of the transition amplitude; dashed curves: transition amplitude includes higher-order contributions in the projectile-electron interaction; solid curves: full calculation including all higher order contributions.

Qualitatively good agreement was found between the experimental data and sophisticated time-dependent *ab initio* calculations [41,45]. In this approach, the projectile

coherence properties were accounted for by representing the projectile as a wave packet, where the width reflects the coherence length. Three different variations of this approach were implemented. In case of the dotted curves in Figure 1.4, only a single interaction between the projectile and the active electron is accounted for (first-order calculation). In case of the dashed curves, the model accounted for higher-order contributions in the projectile- electron interaction (referred to as post-collision interaction or PCI), but higher order contributions involving the projectile-target nucleus interaction (referred as nucleus-nucleus, NN interaction) were not. The solid curves represented full time-dependent calculations, including contributions from both PCI and the NN interaction. The calculations shown by the dotted curves in Figure 1.4, which only represents a pure first order treatment, nevertheless showed pronounced interference structures in the ratios. Thus, the first-order calculations showed that the initial interpretation of single-center interference, by Sharma et al. [39] as being due to interference between first- and higher-order transition amplitudes had to be modified. This calculation demonstrated that single center interference arises primarily due to different impact parameters leading to same scattering angle interfering with each other. Nevertheless, the significant difference between the three sets of calculations shows that although higher order contributions are not essential for single-center interference, they can still play a vital role in the interference term.

Numerous experimental studies, for collision systems involving intermediate energies, have been reported over the past few years supporting an essential role of projectile coherence properties on atomic few body dynamics [31,38,39,40,41,46,47]. Thus, projectile coherence effects can now be regarded as established beyond reasonable

doubt. The primary goal of this dissertation was therefore not to provide further evidence, but rather to use coherence effects as a tool to sensitively study the few- body dynamics of the scattering processes.

To this end, fully differential studies on dissociative single capture and Coulomb explosion through double capture in 75keV p + H_2 collisions were performed. In the former process the projectiles capture an electron from the target molecule, which thereby gets neutralized, and at the same time the molecule breaks up into a positively charged and a neutral fragment. The dissociation of a hydrogen molecule due to single capture can proceed through an electronic transition to a repulsive state as well as by vibrational excitation of the nuclear motion. In the other process investigated in this dissertation, double capture, the projectiles capture both electrons from the hydrogen molecule; therefore, leading to H^- projectile ions. Since both electrons are stripped off from the molecule, now, obviously we are just left with two unscreened protons, which consequently leads to Coulomb explosion.

Three fragmentation channels were studied, which are illustrated in the potential energy diagram of the molecule shown in Figure 1.5. The first channel proceeds through vibrational excitation of the nuclear motion, which is a one-electron process. Here, the projectile captures one electron from the target molecule, which thereby leaves the H_2^+ molecular ion in the electronic ground state, which is a non-dissociative state. The second electron remains passive, and dissociation proceeds through vibrational excitation to a continuum state (red horizontal dashed line in Figure 1.5). This channel corresponds to a small kinetic energy release (KER) of the molecular fragments. The second pathway is a capture of one electron accompanied by excitation of the second electron to a repulsive

electronic state, which is a two-electron process. The green dashed arrow in Figure 1.5 indicates this path. This channel corresponds to relatively large KER. The third path is Coulomb explosion induced by double capture (black dashed arrows in Figure 1.5), which corresponds to an even larger KER then in the previous process. At the same time, an H^- projectile ion is generated.

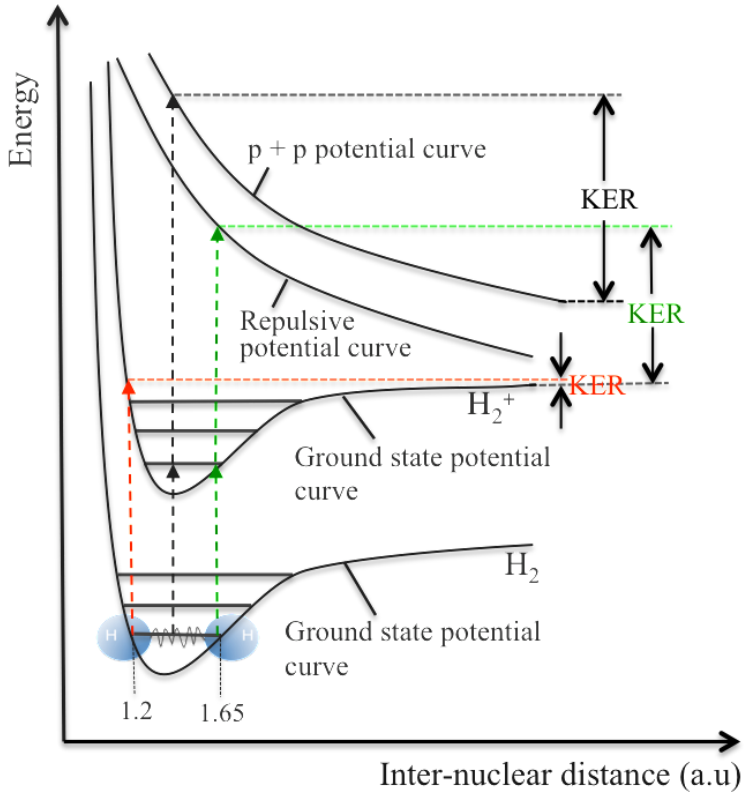

Figure 1.5. Energy diagram of hydrogen molecule. Transitions shown by red colors indicate vibrational dissociation, green color indicates dissociation due to electronic transitions, and black color indicates Coulomb explosion due to double capture.

FDCS were measured and analyzed for coherent and incoherent projectile beams for the fragmentation channels described above. The analysis was focused on the ratio between coherent and incoherent FDCS because it represents the interference term, which

provides sensitive information about the few-body dynamics. We studied the FDCS and the ratios for two different orientations of the molecule; both are perpendicular to the projectile beam axis, but one is also perpendicular to the transverse component of momentum transfer (q_{tr}) while the other is parallel to q_{tr} (See a top panel of Figure1 in the Paper I p.24). The results of my thesis research were published in two journal articles. In the first article, a fully differential study for single electron capture accompanied by vibrational dissociation was reported. The second article focused on fully differential cross sections for single electron capture accompanied by excitation of the second electron to a repulsive state, as well as double electron capture due to Coulomb explosion.

PAPER

I. FULLY DIFFERENTIAL STUDY OF CAPTURE WITH VIBRATIONAL DISSOCIATION IN P + H_2 COLLISIONS

B.R. Lamichhane[1], T. Arthanayaka[1], J. Remolina[1], A. Hasan[1,2], M.F. Ciappina[3], F. Navarrete[4,5], R.O. Barrachina[4,5], R.A. Lomsadze[1,6], and M. Schulz[1]

[1]*Dept. of Physics and LAMOR, Missouri University of Science & Tech., Rolla, MO 65409*

[2]*Dept. of Physics, UAE University, P.O. Box 15551, Al Ain, Abu Dhabi, UAE*

[3]*Institute of Physics of the ASCR, ELI-Beamlines, Na Slovance 2, 182 21 Prague, Czech Republic*

[4]*Centro Atómico Bariloche and Instituto Balseiro (Comisión Nacional de Energía Atómica and Universidad. Nacional. de Cuyo), Bariloche, Río Negro, Argentina*

[5]*Consejo Nacional de Investigaciones Científicas y Técnicas (CONICET), Argentina*

[6]*Tbilisi State University, Tbilisi 0179, Georgia*

ABSTRACT

We have measured fully differential cross sections for electron capture in 75 keV p + H_2 collisions with subsequent dissociation of the intermediate molecular H_2^+ ion by vibrational excitation using different projectile coherence lengths. Data were obtained for two molecular orientations as a function of projectile scattering angle. Two types of interference, single- and molecular two-center interference were identified. The two-center interference structure is phase-shifted by π compared to what we expected. Furthermore, the presence of projectile coherence effects could be reconfirmed.

One of the most important goals of studies on atomic fragmentation processes is to advance our understanding of the few-body problem (FBP) [e.g. 1,2]. The essence of the FBP is that the Schrödinger equation is not analytically solvable for more than two mutually interacting particles even when the underlying forces are precisely known. Therefore, elaborate numerical models have to be developed for its theoretical analysis, and the approximations entering in these models need to be tested by detailed experimental data. To this end, numerous kinematically complete experiments on atomic fragmentation processes induced by charged particle impact have been performed (for reviews see e.g. [3,4]).

The most basic fragmentation process in ion-atom collisions is single ionization of the target. For this process, the essential primary interaction occurs between the projectile and a target electron. In fact, it is remarkable how well the basic features observed in measured cross sections can qualitatively be reproduced by theories which completely ignore the interaction between the nuclei (NN interaction) of the collision partners, especially for small perturbation parameters (projectile charge to speed ratio $\eta = Q_p/v_p$), e.g., Refs. [5-7]. Nevertheless, in order to obtain good quantitative agreement between experiment and theory it is quite important to account for the NN interaction, especially at large values of η, e.g., Refs. [8,9]. However, this interaction usually only plays a "passive" role in inelastic processes in so far as it does not directly cause a target fragmentation by actively triggering an electronic transition. Such a process is not impossible; for example, the projectile could undergo a head-on collision with the target nucleus causing it to recoil at such a large speed that it cannot be followed by the electron. But the cross section for this mechanism is negligibly small.

For molecular targets, the role of the NN interaction in the collision dynamics can be qualitatively different from atomic targets because not only are the electrons bound inside the molecule, but the atoms are also bound to each other. As a result, additional inelastic channels, not present for atomic targets, like e.g. dissociation, are opened for molecular targets. Dissociation can proceed through an electronic transition to a repulsive state, but it can also be caused by vibrational excitation of the nuclear motion (e.g., Refs. [10]), in which the NN interaction can play an active role. Fully differential studies of dissociative processes induced by ion or electron impact are rare. Three kinematically complete experiments on dissociative capture of H_2 or H_2^+, two of them using reversed kinematics, were performed for atom/ion impact [11-13]. In two of them, dissociation by electronic transitions was investigated. In the other, the interest was focused on the nuclear wavefunctions of the molecule for different vibrational states and no fully differential cross sections (FDCS) were reported. FDCS for dissociation of H_2 by vibrational excitation, accompanied by target ionization, were measured for electron impact [14]. There, the interest was focused on advancing the understanding of molecular two-center interference arising from indistinguishable diffraction of the projectile from the two atomic centers of the molecule. To the best of our knowledge, no measured FDCS for dissociative processes through vibrational excitation induced by ion impact have been reported yet.

Another important aspect of collisions with molecular targets that was extensively discussed in recent years is a potential influence of projectile coherence effects on the collision dynamics (e.g., Refs. [15-20]). Experiments were performed for different transverse coherence lengths of the projectiles by placing a collimating slit at varying distances before the target region. Interference structures were present for a large coherence

length, but (nearly) absent for a small coherence length. Earlier, a similar dependence of the interference visibility on the coherence length was studied for Ar atoms interacting with a standing light wave [21]. Later, such effects were also observed for atomic targets [22-24]. In another recent experimental study, performed for a collision system corresponding to small η, no significant differences in the cross sections for varying coherence lengths were found [25]. However, there the coherence lengths were several orders of magnitude larger than the small coherence length studied in [22] for a very similar η and larger than the size of the target atom. Therefore, for small η the question of the role of coherence effects is not conclusively settled yet and further experimental and theoretical work is needed. In contrast, for η close to unity by now there is an extensive literature on both experimental and theoretical studies, e.g., Refs. [15-18,20,26,27] supporting the interpretation that scattering cross sections can be significantly affected by the projectile coherence properties. In this regime, experimental studies now enter a phase in which such coherence effects can be used as a tool to sensitively investigate the few-body reaction dynamics.

In this Letter, we report the first measured FDCS for capture accompanied by dissociation of H_2 through vibrational excitation by proton impact. The data provide additional support for the presence of projectile coherence effects. More importantly, by analyzing the ratios between the FDCS for coherent and incoherent projectiles interference structures could be investigated very sensitively. Two types of interference, single- and two-center interference, were identified. In the latter, an unexpected phase shift in the interference pattern was observed.

The experiment was performed at the accelerator laboratory at Missouri University of Science & Technology. A 75 keV proton beam was passed through vertical and horizontal collimating slits each with a width of 150 μm. The horizontal slit (y-slit) was placed at a distance L_1 = 50 cm and the vertical slit (x-slit) at a distance L_2 = 6.5 cm from the target. These slit geometries correspond to coherence lengths of $\Delta y \approx 3.3$ a.u., and $\Delta x \approx 1.0$ a.u. respectively (see Ref. [17] for a more detailed analysis of the coherence lengths at different L). After traversing the target region, the projectiles were charge-state analyzed by a switching magnet and the neutralized beam component was detected by a two-dimensional position sensitive multi-channel plate detector. From the position information the polar scattering angle θ_p could be determined separately for scattering in the x- and y-directions, i.e., cross sections were recorded for projectiles with a small and a large coherence length simultaneously under identical experimental conditions.

A cold H_2 target beam (T ≈ 1-2 K) was generated with a supersonic gas jet and intersected the projectile beam. This temperature corresponds to thermal energies small compared to rotational and vibrational excitation energies. A capture process in the collision could lead to either an H_2^+ recoil ion or, if accompanied by dissociation, to two molecular fragments, of which at least one must be a proton. The charged recoil ions were extracted by an electric field of about 50 V/cm and detected by a two-dimensional position sensitive multi-channel plate detector, which was set in coincidence with the projectile detector. In the coincidence time spectrum, the H_2^+ ions and protons are represented by separate peak structures due to their mass-dependent time of flight. The shape of each peak contains the momentum information in the direction of the extraction field. The other two momentum components are obtained from the position information. The momentum of the

undetected molecular fragment is determined by momentum conservation. Finally, the kinetic energy release (KER) in the dissociation was calculated from the momenta of the fragments.

FDCS for dissociative capture were extracted for a fixed KER value of 0 - 2 eV and for various fixed molecular orientations as a function of θ_p. Such a small KER value selects events in which the dissociation is caused by vibrational excitation of the molecule rather than by a transition of the second target electron to a repulsive state, e.g. Refs. [10,14]. For each orientation FDCS were obtained for incoherent and coherent projectiles by setting conditions on scattering in the x- and y-directions, respectively. In Figure 1, these FDCS are shown for two molecular orientations, illustrated in the top panels of Figure 1, both of which are perpendicular to the initial projectile beam axis. One orientation (upper left panel) is perpendicular also to the transverse component of the momentum transfer q_{tr} while the second orientation is parallel to q_{tr} (upper right panel). For simplicity, in the following we refer to these orientations as the perpendicular and parallel orientations, respectively. The open symbols represent the incoherent and the closed symbols the coherent FDCS.

Some differences between the various data sets can be seen. The θ_p - dependence of the FDCS for the perpendicular orientation is narrower than the one for the parallel orientation. As a result, statistically significant data could only be obtained up to about 2.5 mrad, while for the parallel orientation this range extends to about 6 mrad. Furthermore, in the coherent data for the perpendicular orientation we observe a structure at small θ_p which is missing in the incoherent data and in both data sets for the parallel orientation: the coherent FDCS are above the incoherent FDCS for small θ_p, they cross the latter near θ_p = 0.3 mrad, reach a shallow minimum at about θ_p = 0.9 to 1.0 mrad, and approach the incohe-

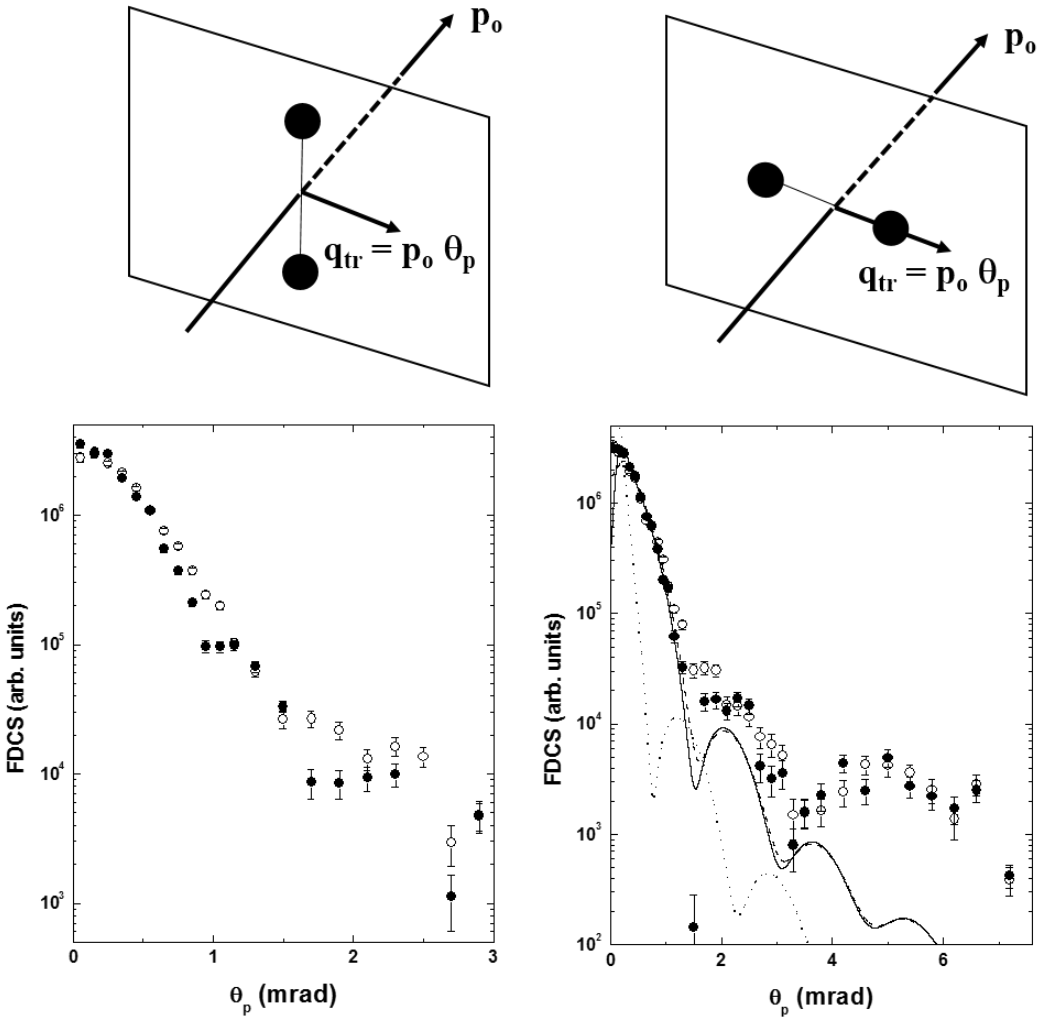

Figure 1. Fully differential cross sections (lower panels) for dissociative capture leading to KER = 1 ± 0.5 eV and for the two molecular orientations illustrated in the top panels as a function of scattering angle measured with incoherent (open symbols) and coherent (closed symbols) projectiles. Both molecular orientations are perpendicular to the beam axis, but one (left panels) is also perpendicular to the transverse component of the momentum transfer $q_\perp$ while the other (right panels) is parallel to $q_\perp$. Dotted curve, coherent eikonal calculation with $\delta = 0$ in the two-center interference term; dashed (solid) curves, incoherent (coherent) eikonal calculations with $\delta = \pi$ in the two-center interference term.

rent FDCS again near $\theta_p = 1.2$ mrad. It is not clear whether the two data points below and above 1.75 mrad represent another minimum or just statistical fluctuations.

For the parallel orientation significant differences between the incoherent and coherent data sets are only discernable for $\theta_p > 1.0$ mrad. For this latter orientation

significant structures are found at large θ_p suggesting interference minima at about 1.5 and 3.2 mrad and maxima around 2.2 and possibly at 4.8 mrad. These structures are also present in the incoherent data; however, they are significantly more pronounced in the coherent case as we will illustrate by analyzing the coherent to incoherent cross section ratios.

The oscillations in the FDCS are more prominent in the ratio R between the coherent and incoherent FDCS, which is plotted for the perpendicular orientation ($R_\perp$) in the top panel of Figure 2. These ratios represent the interference term; however, it is not self-evident what type of interference is reflected by the oscillations. The phase angle in two-center interference is given by $\mathbf{p_{rec}}\cdot\mathbf{D}$, where for a capture process the recoil ion momentum $\mathbf{p_{rec}}$ is equal to $\mathbf{q}$, and $\mathbf{D}$ is the internuclear separation vector in the molecule, e.g., Refs. [12-14]. For the perpendicular orientation this dot product is obviously zero so that here two-center interference cannot lead to any structure in R. We therefore interpret the oscillations observed for the perpendicular orientation as being caused by single-center interference. There, different (non-observable) impact parameters leading to the same (observable) scattering angle interfere with each other [24].

A simple model single-center interference term was suggested by Sharma et al. [17] as $I_1 = (1 + \alpha \cos(q_{tr}\Delta b)$, where α accounts for a reduction in visibility of the interference due to incomplete coherence even at the large slit distance and due to the experimental resolution. Δb represents an effective impact parameter range contributing to the dissociation process, which we approximate as being independent of q_{tr}. A similar analysis was performed for single capture in energetic p + He collisions [28]. The solid curve in the top panel of Figure 2 shows a best fit of the single-center interference term to the measu-

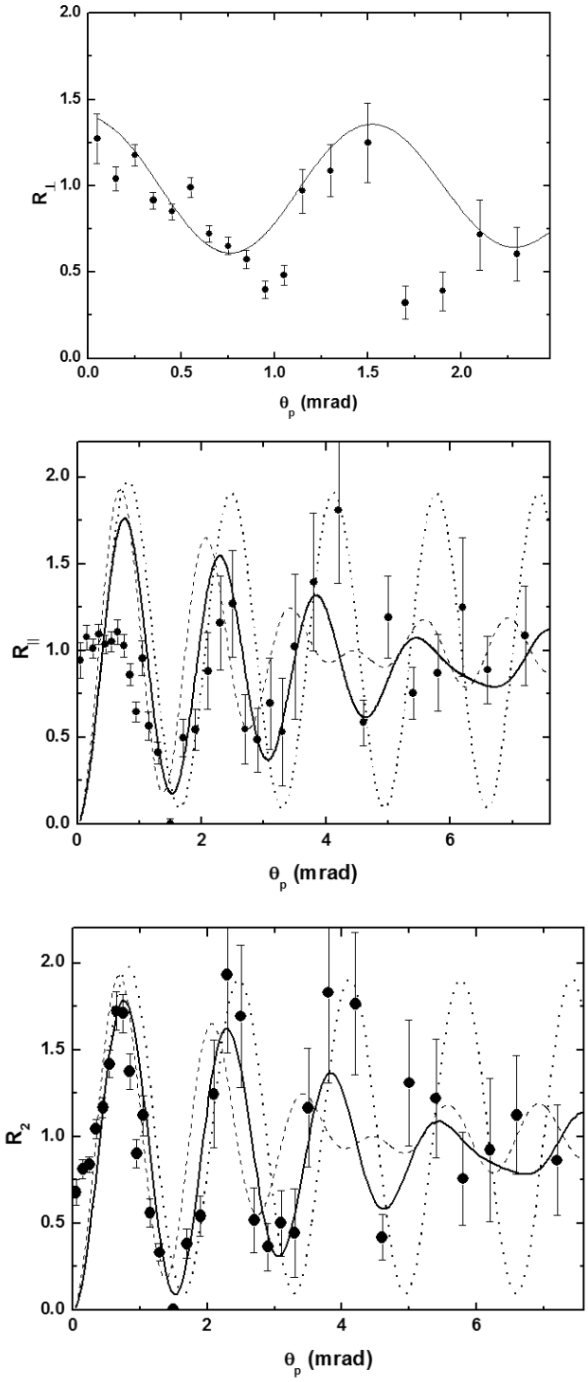

Figure 2. Top panel; ratios $R_\perp$ between the coherent and incoherent FDCS of Figure 1 for the perpendicular orientation. The solid curve shows I_1 calculated for $\Delta b = 1.3$ a.u. Center panel; ratios $R_\parallel$ between the coherent and incoherent FDCS of Figure 1 for the parallel orientation. Bottom panel; double ratios $R_2 = R_\parallel/R_\perp$. The curves in the center and right panels show the two-center interference term for $\delta = \pi$ and D = 1.2 a.u. (dotted curve), averaged over all D assuming equal weights (dashed curve), and averaged over all D with a weight factor decreasing with increasing D (solid curve) (see text).

red ratios yielding $\alpha = 0.4$ and $\Delta b = 1.3$ a.u. This value of Δb appears to be a reasonable reflection of the effective dimension of the diffracting object. However, we emphasize that because of the approximations entering in this analysis it represents only a crude estimate.

The center panel of Figure 2 shows the coherent to incoherent FDCS ratios for the parallel orientation $R_{\|}$. As seen already in the FDCS in Figure 1, $R_{\|}$ is nearly flat up to about 0.8 to 1.0 mrad. However, at larger θ_p, between approximately 1 and 4 mrad, pronounced oscillations are observed, which shows that indeed the structures in the coherent FDCS are significantly more pronounced than in the incoherent FDCS, as mentioned earlier. Both single- and two-center interference can contribute to this orientation so that we would expect $R_{\|}$ to be determined by a product of both interference terms $I_1 I_2$. We make the approximation that Δb is the same for the parallel as for the perpendicular orientation, which is not necessarily the case. With that assumption we obtain the two-center interference term I_2 as the ratio $R_2 = R_{\|}/R_{\perp}$, which is plotted in the bottom panel of Figure 2. In these double ratios the oscillating pattern extends to angles smaller than 1 mrad. The nearly flat behavior of $R_{\|}$ at small θ_p can now be understood as a compensation between single- and two-center interference. While single-center interference alone would make $R_{\|}$ drop with θ_p increasing from 0, two-center interference alone would make it increase.

A striking feature of the θ_p-dependence of R_2 is that there is a minimum at $\theta_p = 0$, while the two-center interference term $I_2 = 1 + \alpha \cos(q_{tr}D)$ predicts a maximum. This minimum suggests that there may be a shift of π in the phase angle of the interference term. The dotted curve in the bottom panel of Figure 2 shows the two-center interference term I_2 with a phase shift of π incorporated. Here, we used 1.2 a.u. instead of the equilibrium

distance of 1.4 a.u. for D because vibrational dissociation mostly occurs near the inner turning point [14], i.e. at the minimum distance in the Franck-Condon region $D_{min} \approx 1.2$ a.u. [29]. Reasonably good agreement with R_2 is achieved; however, the calculated interference term appears to be slightly (but systematically) shifted to larger θ_p. This shift is expected because although vibrational dissociation occurs mostly at the inner turning point, the contributions from other D within the Franck-Condon region are not necessarily negligible. We therefore also calculated I_2 averaged over the entire Franck-Condon region. The dashed curve shows this calculation (unrealistically) assuming that all D contribute equally. Now, with increasing θ_p, I_2 is increasingly shifted to smaller θ_p. This is not surprising either because the influence of large D on the interference term is now overestimated. The actual distribution of D contributing to vibrational dissociation is not known. However, the comparison between the data and the dotted and dashed curves suggest that the data may be reproducible by some distribution in between the extremes of only a single-valued (at D = 1.2 a.u.) and a uniform distribution of D. As an example, the solid curve in the center and bottom panels shows I_2 averaged over the Franck-Condon region giving each D a weight $f = (3.4 - 2D)^2$, so that f = 1 for D = 1.2 a.u. and f = 0.01 for D = 1.65 a.u. (outer turning point). This calculation is in very good agreement with the measured R_2. The deviation seen in $R_{||}$ at small θ_p is due to the contributions from single-center interference. This shows that our data are consistent with the assumption that vibrational dissociation occurs mostly at the inner turning point and falls off with increasing D; but by no means does it prove that f represents the correct distribution of D. Most importantly, the data cannot even be remotely reproduced by I_2 for any distribution

of D within the Franck-Condon region if the phase shift of π is not included, in which case minima and maxima would be reversed compared to the measured data.

It should be noted that even the very small KER value analyzed here is still much larger than typical rotational energies of the molecule (which are of the order of meV). Therefore, the axial recoil approximation (ARA) should be valid, meaning that the momentum direction of the detected fragment does reflect, to a good approximation, the molecular orientation at the instance of the collision. This is confirmed by our measured cross sections as a function of the molecular orientation (see Figure 3), which exhibit maxima parallel and antiparallel to the projectile direction and a minimum perpendicular to it. If the ARA would be significantly violated this angular dependence would be flat. If the ARA is valid, then without any phase shift a maximum should be observed perpendicular to the projectile direction and minima parallel and antiparallel to it. Therefore, our measured orientation-dependent cross sections further confirm the presence of a π phase shift.

The same phase shift was also reported for dissociative capture [11] and excitation [30] data for H_2^+ + He collisions. In both cases the phase shift was explained by a change of symmetry in the electronic state during the transition. However, no phase shift was found in dissociative capture in p + H_2 collisions [13,31]. The authors argued that this showed that the dominant dissociation channel was one where the first electron is captured from a symmetric molecular state while the second electron is excited to a molecular ungerade state. On the other hand, based on the symmetry arguments given in [11] a phase shift of π would be expected in this case. At the same time, a shift of the interference pattern was observed in dissociative ionization by electron impact [14], where no change

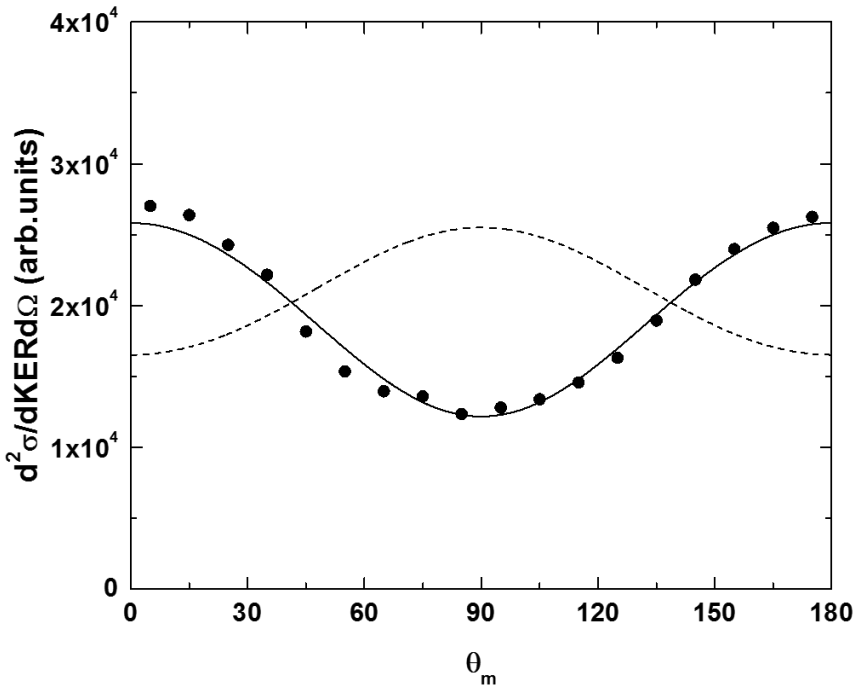

Figure 3. Plot of differential dissociative capture cross sections as a function of the molecular orientation relative to the projectile beam axis.

of symmetry in the electronic state occurs, like in the present data. Nevertheless, the shift of the interference pattern was reproduced by a distorted wave calculation [14], in which the interference term is included from first principles. Therefore, a comprehensive evaluation of these experimental and theoretical results suggests that the two-center interference pattern is not fully understood yet: while two data sets ([11] and [30]) are consistent with a π phase shift due to a change in symmetry in the electronic state, at least three data sets ([13,14] and the present data) appear to behave exactly opposite to the expectation based on the symmetry of the electronic state. Therefore, apart from the electronic symmetry there appear to be other causes that can lead to a phase shift in the interference term.

We have calculated the FDCS for the parallel orientation using a molecular eikonal approach. This method was described in detail previously and successfully reproduces FDCS for single-capture in 75 keV p+H_2 collisions [32]. Conceptually, all interactions are accounted for, including the NN interaction, and treated fully quantum-mechanically. Since the molecular target wave function is modeled in terms of atomic states, two-center interference is not included directly. Rather, it is incorporated by multiplying the cross sections with the interference term $I_2 = 1 + \cos(q_{tr}D + \delta)$ (see e.g. [32,33]) averaged over the Franck-Condon region using the same weight factor f as for the curve in the right panel of Figure 2. The projectile coherence properties are accounted for using the method of Sarkadi et al. [20], i.e. by describing the projectiles in terms of a Gaussian wave packet, where the width reflects the coherence length.

The dotted curve in the right panel of Figure 1 shows this calculation for the parallel orientation, a coherence length of 3.3 a.u., and $\delta = 0$. It is in very poor agreement with the experimental data. However, the same calculation with a phase shift of $\delta = \pi$ is in excellent agreement up to scattering angles of about 1.2 mrad (except for $\theta_p < 0.1$ mrad, which is smaller than the angular resolution) for the coherent case (solid curve) and up to 1.0 mrad for the incoherent case (dashed curve). Between approximately 1.2 and 3.5 mrad the calculation reproduces the location of the oscillation extrema rather well, however, it systematically underestimates the magnitude of the FDCS. Only for angles larger than 3.5 mrad is the agreement between experiment and theory poor. We also note that theory agrees with experiment that even for the incoherent case a structure is visible in the FDCS, which is, however, weaker than in the coherent case. This reflects that the interference

visibility does not abruptly drop to zero once the coherence length drops below the dimension of the diffracting object, but rather this is a smooth transition.[2]

The remaining discrepancies between experiment and theory at angles larger than about 3.5 mrad are at present not understood. We note that for intermediate and large energy ion impact to the best of our knowledge fully differential calculations have never been tested at scattering angles corresponding to such large momentum transfers ($q_x > 11$ a.u.) for any inelastic process.

In conclusion, we have measured fully differential cross sections for capture accompanied by dissociation through vibrational excitation. In the FDCS for fixed molecular orientations as a function of scattering angle we identified molecular two-center interference as well as single center interference between different impact parameters leading to the same scattering angle. Our data are qualitatively consistent with a molecular eikonal calculation, which assumes a phase shift of π in the two-center interference term. However, the origin of this phase shift is currently not understood. Furthermore, at large scattering angles there are significant quantitative discrepancies between experiment and theory. Therefore, further theoretical studies are needed, which should treat two-center interference from first principles. Finally, projectile coherence effects, previously observed in other processes, were confirmed.

---

[2] In fact, according to the van Zittert – Zernicke theorem the visibility reappears in an oscillatory manner, although with reduced amplitude, as the coherence length is further decreased.

This work was supported by the National Science Foundation under grant no. PHY-1401586, by Universidad Nacional de Cuyo (Argentina) under grant 06/C480, and by the project ELI-Extreme Light Infrastructure-phase 2 (Project No. CZ.02.1.01/0.0/0.0/15_008/0000162) from the European Regional Development Fund.

REFERENCES

[1] M. Schulz, R. Moshammer, D. Fischer, H. Kollmus, D.H. Madison, S. Jones, and J. Ullrich, Nature 422, 48 (2003)

[2] T. Rescigno, M. Baertschy, W.A. Isaacs, and C.E. McCurdy, Science 286, 2474 (1999)

[3] A. Lahmann-Bennani, J. Phys. B 24, 2401 (1991)

[4] M. Schulz and D.H. Madison, Intern. J. Mod. Phys. A 21, 3649 (2006)

[5] D. Madison, M. Schulz, S. Jones, M. Foster, R. Moshammer, and J. Ullrich, J. Phys. B 35, 3297 (2002)

[6] M. McGovern, C.T. Whelan, and H.R.J. Walters, Phys. Rev. A 82, 032702 (2010)

[7] K.A. Kouzakov, S.A. Zaytsev, Y.V. Popov, M. Takahashi, Phys. Rev. A 86, 032710 (2012)

[8] M. Foster, D.H. Madison, J.L. Peacher, M. Schulz, S. Jones, D. Fischer, R. Moshammer, and J. Ullrich, J. Phys. B 37, 1565 (2004)

[9] M. F. Ciappina, W. R. Cravero, and M. Schulz, J. Phys. B 40, 2577 (2007)

[10] A. K. Edwards, R. M. Wood, J.L. Davis, and R. L. Ezell, Phys. Rev. A 42, 1367 (1990)

[11] L. Ph. H. Schmidt, S. Schössler, F. Afaneh, M. Schöffler, K. E. Stiebing, H. Schmidt-Böcking, and R. Dörner, Phys. Rev. Lett. 101, 173202 (2008)

[12] L. Ph. H. Schmidt, T. Jahnke, A. Czasch, M. Schöffler, H. Schmidt-Böcking, and R. Dörner, Phys. Rev. Lett. 108, 073202 (2012)

[13] H.T. Schmidt et al., Phys. Rev. Lett. 101, 083201 (2008)

[14] A. Senftleben, T. Pflüger, X. Ren, O. Al-Hagan, B. Najjari, D. Madison, A. Dorn, and J. Ullrich, J. Phys. B 43, 081002 (2010)

[15] K.N. Egodapitiya, S. Sharma, A. Hasan, A.C. Laforge, D.H. Madison, R. Moshammer, and M. Schulz, Phys. Rev. Lett. 106, 153202 (2011)

[16] S. Sharma, A. Hasan, K.N. Egodapitiya, T. P. Arthanayaka, and M. Schulz, Phys. Rev. A 86, 022706 (2012)

[17] S. Sharma, T.P. Arthanayaka, A. Hasan, B.R. Lamichhane, J. Remolina, A. Smith, and M. Schulz, Phys. Rev. A 90, 052710 (2014)

[18] T.P. Arthanayaka, S. Sharma, B.R. Lamichhane, A. Hasan, J. Remolina, S. Gurung, and M. Schulz, J. Phys. B 48, 071001 (2015)

[19] J.M. Feagin and L. Hargreaves, Phys. Rev. A 88, 032705 (2013)

[20] L. Sarkadi, I. Fabre, F. Navarrete, and R. Barrachina, Phys. Rev. A 93, 032702 (2016)

[21] C. Keller, J. Schmiedmayer, and A. Zeilinger, Opt. Comm. 179, 129 (2000)

[22] X. Wang, K. Schneider, A. LaForge, A. Kelkar, M. Grieser, R. Moshammer, J. Ullrich, M. Schulz, and D. Fischer, J. Phys. B 45, 211001 (2012)

[23] K. Schneider, M. Schulz, X. Wang, A. Kelkar, M. Grieser, C. Krantz, J. Ullrich, R. Moshammer, and D. Fischer, Phys. Rev. Lett. 110, 113201 (2013)

[24] T. Arthanayaka, B.R. Lamichhane, A. Hasan, S. Gurung, J. Remolina, S. Borbély, F. Járai-Szabó, L. Nagy, and M. Schulz, J. Phys. B 49, 13LT02 (2016)

[25] K. Gassert et al., Phys. Rev. Lett. 116, 073201 (2016)

[26] F. Navarrete, M.F. Ciappina, L. Sarkadi, and R.O. Barrachina, accepted for publication in Nucl. Instrum. Meth. B (2017)

[27] A. Igarashi and L. Gulyas, J. Phys. B 50, 035201 (2017)

[28] M. Gudmundsson et al., J. Phys. B 43 , 185209 (2010)

[29] T.E. Sharp, At. Data Nucl. Data Tables 2 119 (1970)

[30] S.F. Zhang, D. Fischer, M. Schulz, A.B. Voitkiv, J. Ullrich, X. Ma, and R. Moshammer, Phys. Rev. Lett. 112, 023201 (2014)

[31] K. Støchkel et al., Phys. Rev. A 72, 050703 (2005)

[32] E. Ghanbari-Adivi, and S.H. Sattarpour, Mol. Phys. 113, 3336-3344 (2015)

[33] M.F. Ciappina, and R.D. Rivarola, J. Phys. B 41, 015203 (2008)

II. FULLY DIFFERENTIAL STUDY OF DISSOCIATIVE SINGLE CAPTURE AND COULOMB EXPLOSION THROUGH DOUBLE CAPTURE IN P + H_2 COLLISIONS

B.R. Lamichhane[1], A. Hasan[1,2], T. Arthanayaka[1], M. Dhital[1], K. Koirala[1], T. Voss[1], R.A. Lomsadze[1,3], and M. Schulz[1]

[1]Dept. of Physics and LAMOR, Missouri University of Science & Technology, Rolla, MO 65409

[2]Dept. of Physics, UAE University, P.O. Box 15551, Al Ain, Abu Dhabi, UAE

[3]Tbilisi State University, Tbilisi 0179, Georgia

ABSTRACT

We have measured fully differential cross sections for dissociative single capture and Coulomb explosion through double capture in 75 keV p + H_2 collisions. Data were analyzed for fixed kinetic energy releases and molecular orientations as a function of scattering angle. Two-center interference was identified for dissociative single capture. The interference pattern is not inconsistent with the symmetry of the dissociative electronic state affecting the phase angle of the interference term. No clear signatures of single-center interference were observed for either process. For double capture at most only a very weak two-center interference structure was found. This very small (or zero) visibility can probably be attributed to a convolution of two independent scatterings of the projectile with the two electrons yielding the measured scattering angle.

1. INTRODUCTION

The basic interest underlying most research on atomic collisions is to advance our understanding of the few-body dynamics of processes occurring in simple atomic systems [e.g., 1-4]. The fundamental difficulty is that the Schrödinger equation is not analytically solvable for more than 2 mutually interacting particles. Therefore, theory has to resort to elaborate numeric modelling efforts. The assumptions and approximations entering in these models have to be tested by detailed experimental data.

Experimental data which exhibit interference structures are particularly suitable to test theoretical models because the interference pattern depends sensitively on the details of the few-body dynamics. An example is molecular two-center interference, which has been observed in numerous experimental studies and predicted by theory for charged particles colliding with diatomic molecules [e.g., 5-20]. There, the diffracted projectile waves originating from the two atomic centers interfere with each other. However, the identification of an interference pattern can be rather challenging. Experiments which integrate over certain kinematic parameters effectively average the cross sections over the phase angle so that the interference structure may be partly or completely "smeared out". If differential cross sections are analyzed as a function of scattering angle the interference pattern is usually superimposed on a steep dependence of the incoherent cross sections on the scattering angle, which can also significantly reduce the visibility of an oscillating pattern.

Pronounced interference structures were found when the momenta of all collision fragments were determined with good resolution [12]. One approach to identify an interference pattern even when it is not or barely visible in the cross sections is to normalize

the cross sections to those one would obtain without the interference term, to which we refer as the incoherent cross section $d\sigma_{inc}$. In analogy to classical optics the cross section including the interference term *I* (coherent cross section) can be expressed as $d\sigma_{coh} = d\sigma_{inc}$ *I* so that *I* is given by the coherent to incoherent cross section ratio R [7-10,13,15,16]. The difficulty with this approach is that until recently it was not clear how $d\sigma_{inc}$ could be experimentally determined. Therefore, $d\sigma_{inc}$ was often approximated as the cross section for two separate H atoms or a He target [7-10,13,15,16]. In R even small differences between the real and approximated incoherent cross sections can lead to artificial structures, which could be misinterpreted as interference structures.

A few years ago, we demonstrated that $d\sigma_{inc}$ can be experimentally determined with high accuracy by manipulating the projectile coherence properties by placing a collimating slit in front of the target [17]. If a slit of fixed width is placed at a large distance from the target the local collimation angle subtended by the slit at the target position corresponds to a small momentum spread of the incoming wave, which, in turn, corresponds to a large coherence length Δr. The incoming projectile wave can then coherently illuminate both atomic scattering centers of the molecule simultaneously and interference between the diffracted waves from both centers is observable. Likewise, a small slit distance results in a large local collimation angle, i.e., a large momentum spread, so that the coherence length is not sufficiently large for both atomic centers to be simultaneously illuminated by the projectile wave. In this case no interference is observed. Therefore, the interference term can be accurately determined as the ratio between the cross sections measured for a large and a small slit distance.

The interpretation offered in Ref. [17] was challenged by Feagin and Hargreaves [21], who argued that the differences between the cross sections measured for the large and small slit distances were merely due to differences in the beam divergence. However, this assertion was rebutted by Sharma et al. [22], who demonstrated that there were no noticeable differences in the beam divergence for the two slit distances. Later, resolution-independent coherence effects were reported for various processes and targets for projectiles with relatively small speed and large perturbation parameters η (projectile charge to speed ratio) [19,20,23,24; for a review see Ref. [25]]. Two experimental studies also reported coherence effects for large projectile speeds and atomic targets [26,27], while no such effects were observed [28] for a similar collisions system as investigated in [26]. However, the smallest coherence length realized in [28] was about three orders of magnitude larger than in [26] and larger than the size of the target atom.[3] Therefore, no significant coherence effects were expected, as also confirmed by a recent theoretical study [29]. Nevertheless, at small η further experimental and theoretical studies are needed to confirm or disprove such coherence effects.

In contrast, at large η the extensive literature on coherence effects strongly suggests that indeed such effects can play an important role in ion – atom/molecule collisions. Here, research is now entering the next phase in which coherence effects are used as a tool to study the few-body dynamics in more detail. To this end we recently reported measurements of fully differential cross sections (FDCS) for single capture accompanied by vibrational dissociation in $p + H_2$ collisions for various molecular orientations as a

[3] The coherence length reported in Ref. [28] was calculated incorrectly and was too small by about 65%.

function of scattering angle [30]. In this process the second electron stays in the ground state and dissociation proceeds through excitation of the nuclear motion to a vibrational continuum state. By analyzing the coherent to incoherent FDCS ratios we were able to identify single-center and two-center interference simultaneously in the same data set. The former, in which different impact parameters leading to the same scattering angle interfere with each other, can also occur for atomic targets [20,24,25,31]. More importantly, an unexpected shift of π was observed in the phase angle for two-center interference. Such a phase shift was also found for H_2^+ + He collisions and was explained by a switch in the symmetry of the final compared to the initial electronic state [12,16]. However, no such switch in symmetry occurs in vibrational dissociation studied in [30]. Furthermore, the interference patterns observed for double capture [11] and dissociative ionization by electron impact [15] cannot be explained by the electronic symmetry either. These data suggest that there are other factors apart from the electronic symmetry which can lead to (or counteract) a phase shift. This, in turn, implies that the phase angle, and therefore the few-body reaction dynamics, is not fully understood yet.

Here, we report measured FDCS for another dissociative single capture channel, namely capture accompanied by excitation of the second electron to a repulsive electronic state, as well as for Coulomb explosion induced by double capture. We focus on FDCS for a molecular orientation parallel to the transverse component of the momentum transfer **q** (difference between the initial and final projectile momentum). Data were obtained for a kinetic energy release (KER) for which two electronic states of opposite symmetry predominantly contribute to dissociation.

2. EXPERIMENT

The experiment was performed at Missouri University of Science & Technology. The experimental set-up is essentially the same as the one used in Ref. [18] and is shown in Figure 1.

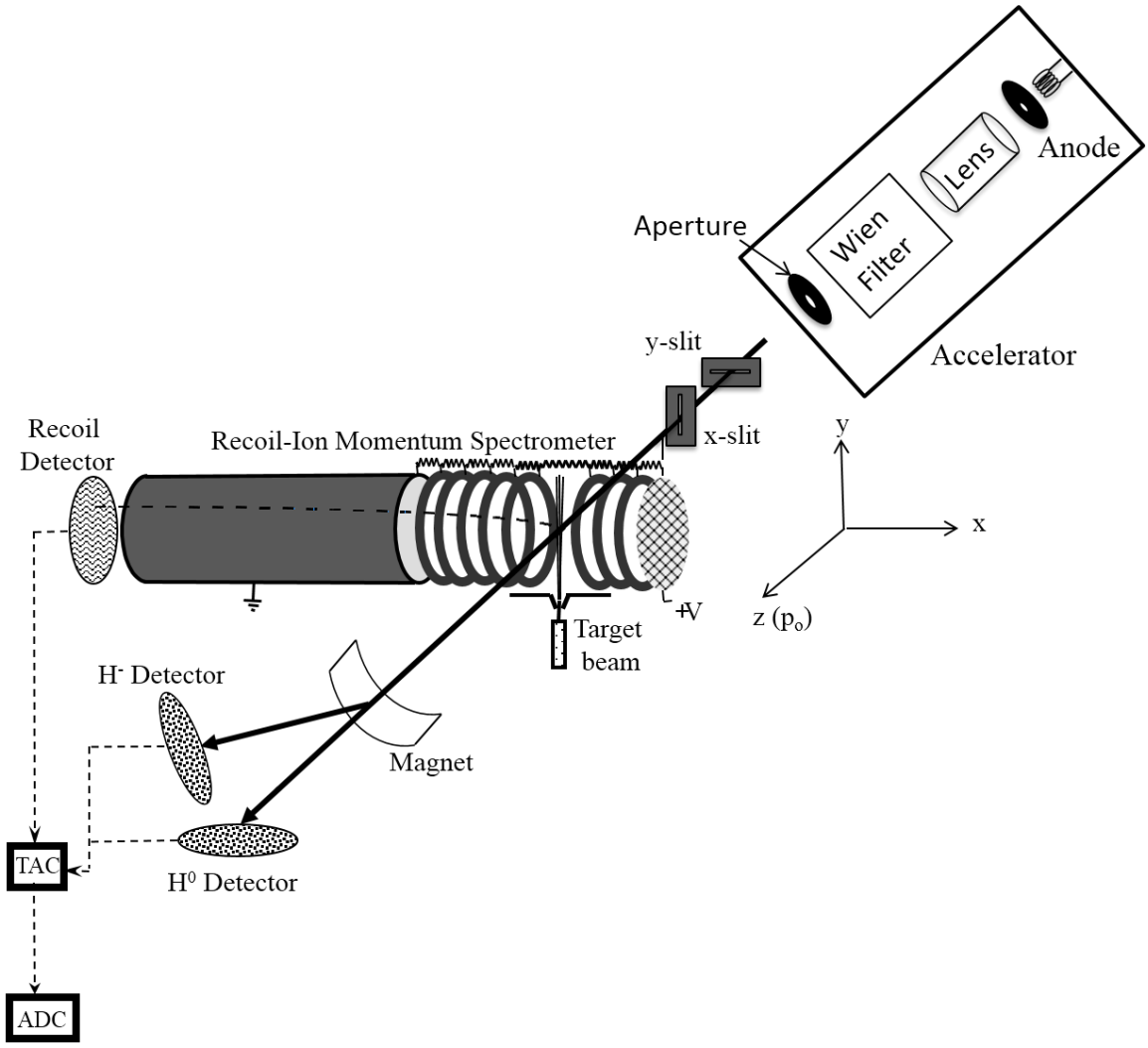

Figure 1. Schematic diagram of the experimental set-up.

A proton beam was generated with a hot cathode ion source and accelerated to an energy of 75 keV. The beam was collimated by a vertical slit (x-slit), placed at a distance from the target of L_1 = 6.5 cm, and a horizontal slit (y-slit), placed at a distance L_2 = 50 cm, both with a width of 150 μm. These slit distances correspond to transverse coherence lengths of Δx = 0.43 a.u. in the x-direction and Δy = 3.3 a.u. in the y-direction. However, in the x-direction the coherence properties are not determined by the collimating slit, but rather by an aperture at the end of the accelerator terminal so that the smaller coherence length is about Δx = 1.0 a.u. [19].

The collimated projectile beam was then crossed with a very cold ($T \approx$ 1-2 K) H_2 beam from a supersonic jet propagating in the y-direction. The molecular proton fragments produced in the collision were extracted by a uniform electric field of 250 (for dissociative single capture) to 350 V/cm (for double capture) pointing in the x-direction and guided onto a two-dimensional position-sensitive channel-plate detector. For dissociative single capture at these field strengths, all proton fragments with energies up to 7.5 eV (i.e., KER = 15 eV) hit the detector. For the double capture experiment, the recoil-ion spectrometer axis was slightly tilted, and the detector slightly moved up compared to the settings for dissociative single capture such that the fragments with small momenta in the plane of the detector were steered from the center towards the lower right corner of the detector. The data were then later analyzed only for the upper left quadrant relative to the position corresponding to a zero momentum. In this way FDCS for double capture could be obtained without suppressing certain orientations relative to others for KER values of up to about 30 eV.

After the target region the projectile beam was charge-state analyzed by a switching magnet. A second two-dimensional position-sensitive channel-plate detector was positioned either at 0^o relative to the initial beam direction, so that the neutralized projectiles were detected (dissociative single capture), or at 45^o, so that H^- projectiles were detected (double capture). The detector was set in coincidence with the molecular fragment detector. From the coincidence time the time of flight of the molecular proton fragments were determined and thereby the momentum component in the direction of the extraction field. The momentum components in the y- and z-directions were obtained from the position information. From the momentum components the molecular orientation and the KER value were calculated. At such a large extraction field the momentum resolution is primarily determined by the size of the interaction volume and by the position and time resolution of the detector [32]. Furthermore, it depends on the momentum itself. For p = 35 a.u. it was about 2 a.u. full width at half maximum (FWHM) for all components resulting in a KER resolution of about 3 eV FWHM. The polar and azimuthal angular resolution in the molecular orientation was about 10^o FWHM.

From the position information of the projectile detector the polar and azimuthal scattering angles were determined. The FDCS for coherent and incoherent projectiles were obtained simultaneously, under otherwise identical experimental conditions, by setting conditions on the azimuthal angle to select scattering in the x-direction (incoherent) or in the y-direction (coherent). The resolution in the polar angle was about 0.15 mrad FWHM and in the azimuthal angle it was very small (3^o FWHM) compared to the entire 360^o range contributing to all dissociation events. However, in order to obtain the FDCS with sufficient statistics the condition on the azimuthal angle had a width of $\pm 15^o$.

3. DATA ANALYSIS

In Figure 2, we show coincidence time spectra for dissociative single capture (left panel) and double capture (right panel). In the case of dissociative capture, a pronounced triple peak structure is visible. A similar shape of the time spectrum was also observed for dissociative ionization in fast p + H_2 collisions [33]. The center peak reflects events in which the molecular proton fragment has a small momentum in the direction of the extraction field. This can be realized either by a small KER value, occurring in dissociation through vibrational excitation [30], or by a molecular orientation in the plane perpendicular to the extraction field. The left maximum is due to fragments which gained a large momentum towards the detector in the dissociation and the right maximum those in which the fragments gained a large momentum away from the detector.

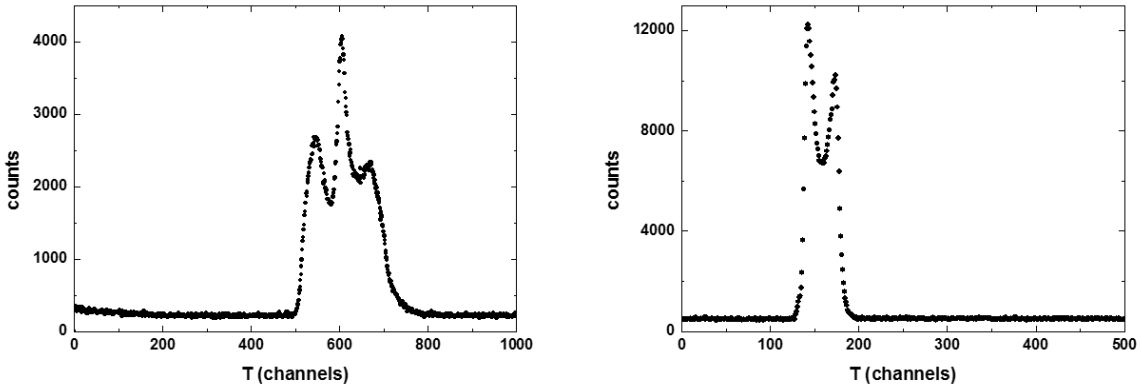

Figure 2. Time spectrum of coincidences between neutralized projectiles and molecular proton fragments (left panel) and H^- projectiles and molecular proton fragments (right panel).

In the time spectrum for double capture the center peak is missing. This can be understood by the fact that here Coulomb explosion, for which small KER values are not

possible, is the only fragmentation channel. Apparently, the contributions from molecules oriented in the plane perpendicular to the extraction field are not large enough to lead to a resolved center peak structure.

In Figure 3 we show KER spectra for three different cases. The closed circles represent dissociative capture measured with a small extraction field of only 50 V/cm. In this case all fragments from molecules oriented in the plane perpendicular to the extraction field with a momentum larger than 14 a.u. (corresponding to KER = 3 eV) miss the detector. As a result, large KER values, resulting from electronic transitions to repulsive states, are strongly suppressed.

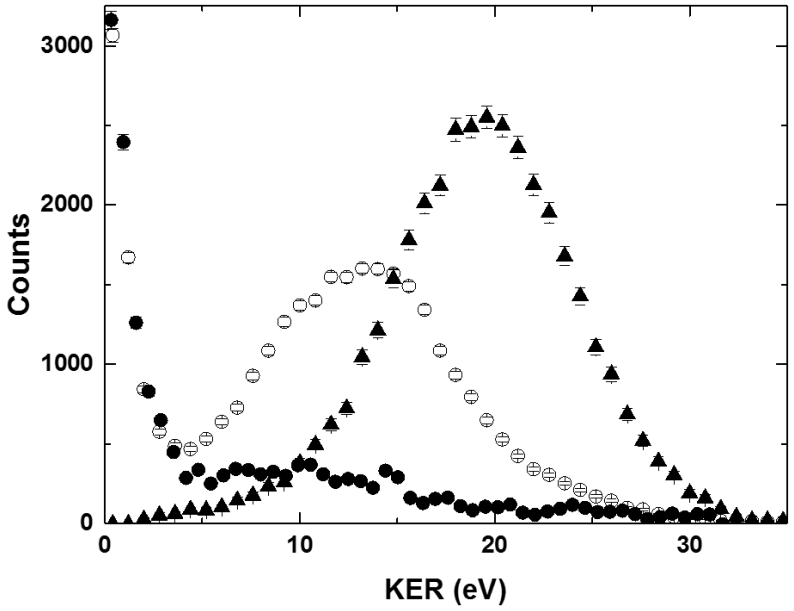

Figure 3. Kinetic energy release (KER) spectrum coincident with H^o projectiles (open and closed circles) and with H^- projectiles (solid triangles). The open (closed) circles were recorded with a large (small) recoil-ion extraction voltage.

The spectrum is dominated by small KER values representing dissociation by vibrational excitation, for which data were reported previously [30]. The open circles

represent dissociative single capture measured with an extraction field of 250 V/cm. Now, all fragments with energies up to 7.5 eV (KER = 15 eV), regardless of orientation, hit the detector. As a result, a pronounced and separate peak structure at 13 eV is observed. Finally, the closed triangles represent double capture measured with an extraction field of 350 V/cm. Now, the small KER component, which is very pronounced for dissociative single capture, is completely absent. Rather, only a single peak structure with the centroid at 19.5 eV, corresponding to the potential energy of the two protons at the equilibrium distance of H_2, is observed.

Earlier, we reported FDCS for a condition on KER = 0 to 2 eV, i.e., for electronic ground state dissociation through vibrational excitation [30]. Here, we analyzed FDCS for dissociative single capture for a condition KER = 5 – 12 eV. In this region contributions to dissociation come mostly from the $2p\pi_u$ and $2s\sigma_g$ states and, to a much lesser extent, from the $2p\sigma_u$ state of H_2^+ [34]. In the case of double capture Coulomb explosion is the only fragmentation channel. Here, the KER value unambiguously determines the internuclear separation D at the instance of the collision as D = 1/KER (in a.u.). Data were analyzed for KER regions of 13-18 eV, 18-22 eV, and 22-27 eV.

In addition to the KER value conditions were also set on the molecular orientation and on the azimuthal projectile scattering angle. FDCS will be presented for two molecular orientations, which are illustrated in Figure 4. Both of them are perpendicular to the projectile beam axis (i.e. the polar molecular angle is centered on $\theta_m = 0^o$). One of them (left panel of Figure 4) is perpendicular also to the transverse component of the momentum transfer q_{tr} (i.e. $\varphi_m = 90^o$) while the second (right panel of Figure 4) is parallel to q_{tr} (i.e. $\varphi_m = 0^o$). For simplicity, in the following we refer to these orientations as the perpendicular

and parallel orientation, respectively. The corresponding conditions in the azimuthal and polar angles of the detected molecular proton fragments had a width of $\Delta\theta_m$ and $\Delta\varphi_m = \pm 15^o$.

To select coherent and incoherent incoming projectiles a condition was also set on the azimuthal projectile scattering angle $\varphi_p = 0^o \pm 15^o$ (scattering in x-direction, incoherent) $\varphi_p = 90^o \pm 15^o$ (scattering in y-direction, coherent). For each KER value four fully differe-

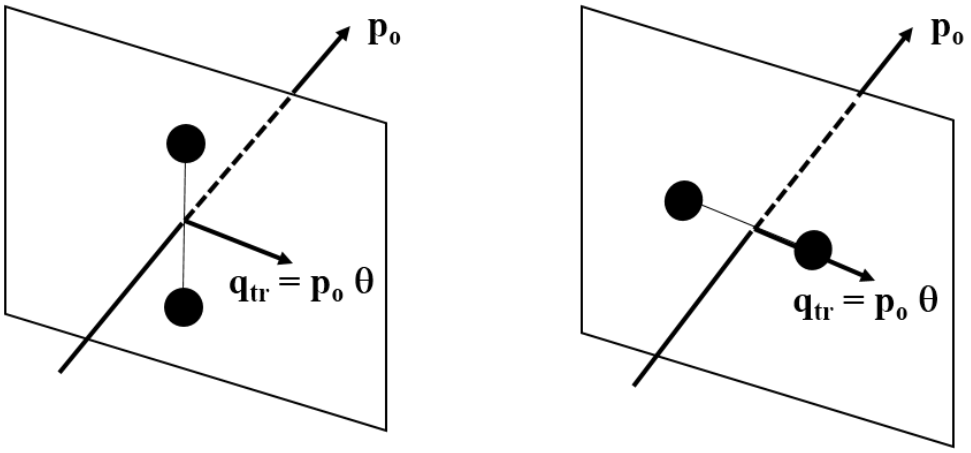

Figure 4. Illustration of the two molecular orientations for which fully differential cross sections were analyzed. The left panel shows the perpendicular and the right panel the parallel orientation (relative to the transverse component of the momentum transfer).

ntial spectra were generated as a function of the polar projectile scattering angle θ_p: 1.) $\varphi_p = 0^o$ and $\varphi_m = 0^o$ (incoherent projectiles, parallel orientation); 2.) $\varphi_p = 0^o$ and $\varphi_m = 90^o$ (incoherent projectiles, perpendicular orientation); 3.) $\varphi_p = 90^o$ and $\varphi_m = 0^o$ (coherent projectiles, perpendicular orientation); 4.) $\varphi_p = 90^o$ and $\varphi_m = 90^o$ (coherent projectiles, parallel orientation).

4. RESULTS AND DISCUSSION

In Figure 5 FDCS are plotted for dissociative single capture for the perpendicular orientation and KER = 5 – 12 eV as a function of θ_p. The open symbols represent the FDCS for the incoherent projectiles and the closed symbols those for the coherent projectiles. Within the statistical fluctuations no significant differences between the coherent and incoherent data can be discerned. The phase angle for two-center interference is determined by the dot product between the internuclear separation vector and the recoil-ion momentum, which for capture is equal to **q**. For the perpendicular orientation this dot product is constant at zero for all θ_p so that no differences between the coherent and incoherent data can be discerned. The phase angle for two-center interference is determined by the dot product between the internuclear separation vector and the recoil-ion momentum, which for capture is equal to **q**. For the perpendicular orientation this dot product is constant at zero for all θ_p so that no differences between the coherent and incoherent FDCS due to two-center interference are expected. However, for KER = 0 – 2 eV, i.e. for dissociative capture through vibrational excitation, we found significant differences caused by single-center interference [30].

One possible explanation for the apparent absence of single-center interference in the present data is that dissociation leading to a large KER requires a two-electron process (capture of one electron and excitation of the second electron to an anti-binding state). At the relatively large η for this collision system the transitions of both electrons are predominantly caused by two independent interactions with the projectile. Therefore, the measured total scattering angle is the result of a convolution of the deflections of the

projectile in these two steps. This convolution is reflected in the scattering angle dependence of the interference term and thus can lead to a loss of visibility.

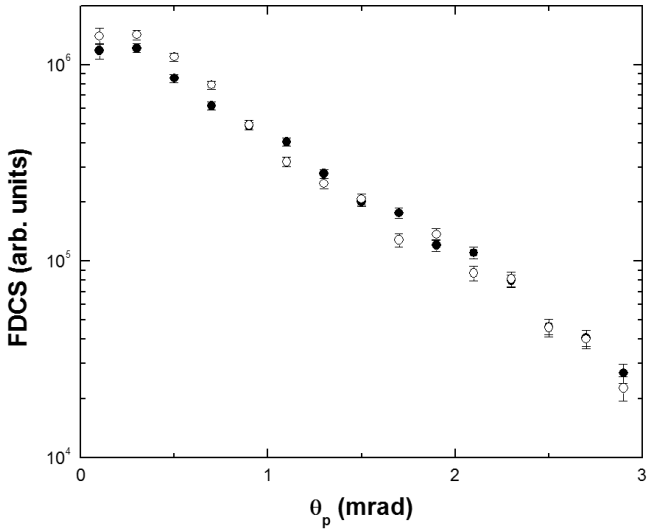

Figure 5. Fully differential cross sections (FDCS) for dissociative capture leading to KER = 5-12 eV and a molecular orientation perpendicular to both the initial projectile beam axis and the transverse component of the momentum transfer as a function of scattering angle. The open (closed) symbols represent the data taken with an incoherent (coherent) projectile beam.

In Figure 6 the FDCS are shown for the parallel orientation under otherwise identical kinematic conditions as in Figure 5. For this orientation we observe some differences between the coherent and incoherent data. Between approximately 0.4 and 1.2 mrad the coherent FDCS lie systematically below the incoherent FDCS, while between 1.3 and 2.1 mrad they are systematically larger. These differences are more clearly visible in the coherent to incoherent FDCS ratios $R_{\|}$, which are plotted in Figure 7, in terms of a departure from $R_{\|} = 1$, especially in the maximum seen at about 1.7 mrad (and possibly a shallow minimum at 0.9 mrad). While this structure is statistically significant, it is not as pronounced as in the case of vibrational dissociation and the interference extrema occur at

different angles [30]. The reason that it is visible at all in spite of the underlying double projectile scattering, in contrast to single-center interference, is probably that for single sc-

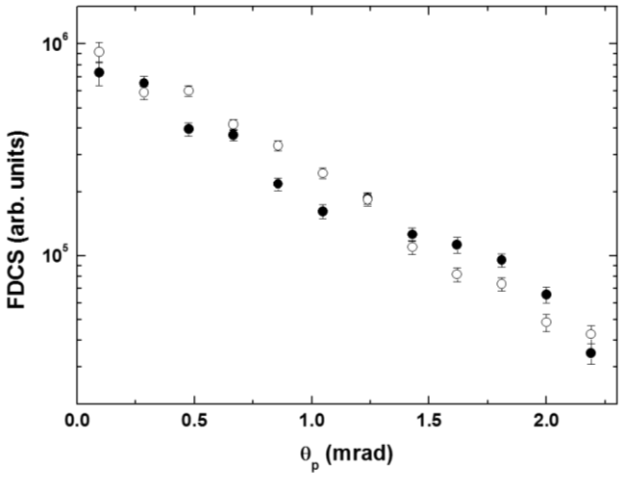

Figure 6. Same as Figure 5, but molecular orientation is parallel to the transverse component of the momentum transfer.

attering (like in, e.g., vibrational dissociation) two-center interference is significantly more pronounced than single-center interference [30]. A two-center interference structure thus has a better chance of partly surviving the convolution over two scatterings.

Given the argument that a switch in the symmetry of the electronic state should lead to a π phase shift in the two-center interference term one might not necessarily had expected a pronounced interference structure in the selected KER regime. The total interference term is a sum of those obtained for the $2p\pi_u$ state, for which a π shift would be expected, and the $2s\sigma_g$ state, for which no phase shift would be expected. Thus, if the contributions from both states would be exactly identical this sum should exhibit no dependence at all on θ_p. However, for electron impact, at the same projectile speed as in our study, Edwards and Zheng demonstrated that the relative cross sections for excitation

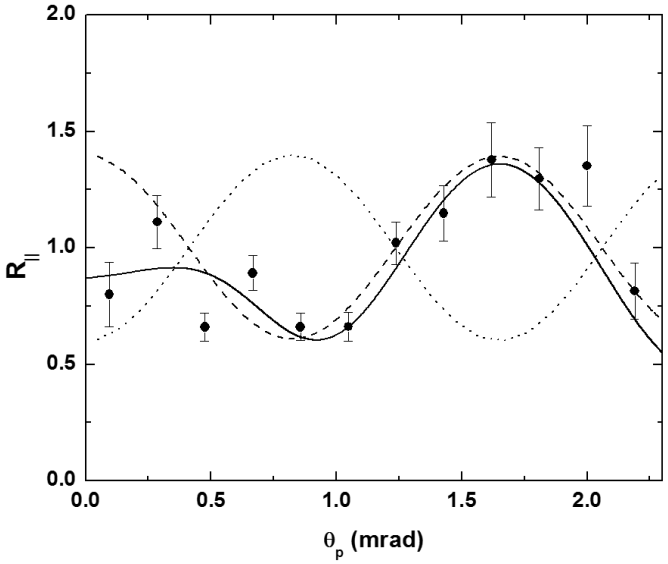

Figure 7. Ratios between the FDCS for coherent and incoherent projectiles from Figure 6 as a function of scattering angle. Dashed curve, two-center interference term expected for a gerade dissociative state; dotted curve, two-center interference term expected for an ungerade dissociative state; solid curve, sum of the dashed and dotted curves with weight factors of f and 1-f for the geared and ungerade states, respectively. For f, see text.

to the $2p\pi_u$ and $2s\sigma_g$ states sensitively depend on the angle θ_{mq} between the molecular axis and **q** [35], which is illustrated in the top panel Figure 8. For small θ_{mq} the $2s\sigma_g$ state is predominantly populated and for large θ_{mq} contributions from the $2p\pi_u$ state are larger.

For the parallel orientation the molecular axis vector **D** and **q** lie in the same plane and the polar molecular angle is fixed at $\theta_m = 90^o$. Therefore, the angle between **q** and the projectile beam axis θ_q and θ_{mq} always add up to 90^o (see Figure 8). Furthermore, θ_q is given by

$$\theta_q = tg^{-1}(q_{tr}/q_z) \qquad (1)$$

where $q_{tr} = p_o \sin(\theta_p)$. Therefore, for this geometry θ_{mq} is unambiguously determined by θ_p as

$$\theta_{mq} = \pi/2 - tg^{-1}(p_o \sin(\theta_p)/q_z) \qquad (2)$$

i.e. large θ_p corresponds to small θ_{mq} and vice versa. Here, the longitudinal component of **q** is given by $q_z = -Q/v_p - v_p/2$, where Q is the Q-value of the reaction and v_p is the projectile speed. The data of Figure 7 are replotted in the bottom panel of Figure 8 as a function of θ_{mq}. In this presentation, a sharp peak structure is seen at about 8°. If the dependence of the relative $2s\sigma_g$ to $2p\pi_u$ population on θ_{mq} is similar as in [35] then this peak structure should be caused by two-center interference without phase shift expected for the $2s\sigma_g$ state. The interference term expected for a gerade state is given by

$$I_2 = 1 + \alpha\cos(\mathbf{q}.\mathbf{D}) \qquad (3)$$

where α, which we call the visibility factor, describes to what extent the interference is "washed out" due to incomplete coherence (even at the large slit distance) and experimental resolution. I_2 calculated for $\alpha = 0.4$, which is plotted as the dashed curve in Figure 7 and Figure 8, is in very good agreement with the experimental data for $\theta_{mq} < 20^o$ and $\theta_p > 0.8$ mrad, respectively. At the same time the same interference term for ungerade states (dotted curve) is in poor agreement with the data. For larger θ_{mq} (smaller θ_p) we have only four data points with relatively large statistical fluctuations so that no conclusions can be drawn. The solid curve represents a sum of the interference terms for the gerade and ungerade states, where each state was given a weight of f and 1-f, respectively. f was obtained by fitting a Woods-Saxon distribution as a function of θ_{mq} to the relative $2s\sigma_g$ to $2p\pi_u$ populations given by Edwards and Zheng [35]. Overall, this combined interference term appears to be consistent with the experimental data in the entire angular range thus supporting the interpretation that a switch in the symmetry of the electronic state has to be compensated by a phase shift in the diffracted projectile wave.

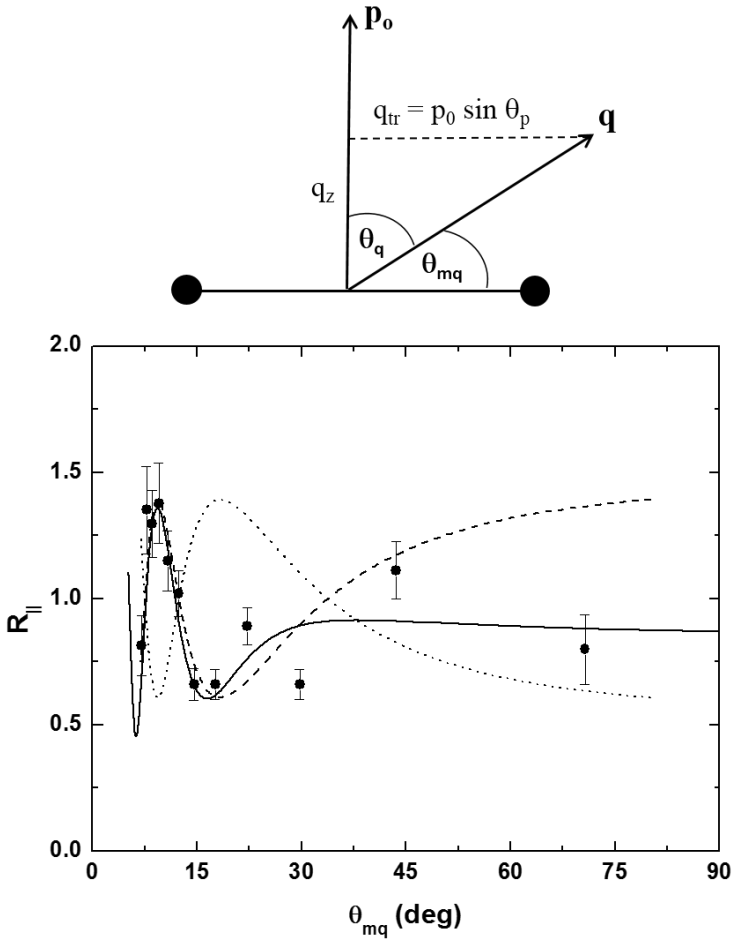

Figure 8. Top panel: illustration of the angle θ_q enclosed by the momentum transfer **q** and the projectile beam axis and of the angle θ_{mq} enclosed by the molecular axis and **q.** Bottom panel: ratios of Figure 7 plotted as a function of the angle between the molecular axis and the momentum transfer vector θ_{mq} calculated with eq. (2). Curves: same as in Figure 7.

One question that still needs to be addressed is why the interference structure is significantly less pronounced than for vibrational dissociation. In addition to the afore-mentioned convolution over the two projectile scatterings off both electrons two other factors may contribute to a loss of visibility of the interference structure. First, the two interference terms for the gerade and ungerade states mutually weaken the structures of the separate terms because they are phase-shifted relative to each other. However, the comparison between the dashed curves and the experimental data in Figure 7 shows that

only for $\theta_p < 0.5$ mrad this has a significant effect. Second, the width of the condition on the KER value corresponds to a range of internuclear distances contributing to the FDCS. As a result, the phase angle in the interference term, **q.D**, is afflicted with some uncertainty. This factor becomes increasingly important with increasing θ_p. In the region of the interference maximum q_{tr} is about 5 a.u. Thus, a spread in D of 0.2 a.u. can cause a spread in the phase angle of about $\pi/3$, which could lead to a significant loss of visibility.

Further information as to which of these three factors is mostly responsible for the damping of the interference structure we obtained from the data on double capture. The cross-section differential in the projectile and molecular solid angles is plotted in Figure 9 and Figure 10 for the perpendicular and parallel orientation, respectively, as a function of θ_p. Hardly any differences between the coherent and incoherent cross sections are discernable for either orientation; i.e. neither single- nor two-center interference can be cle-

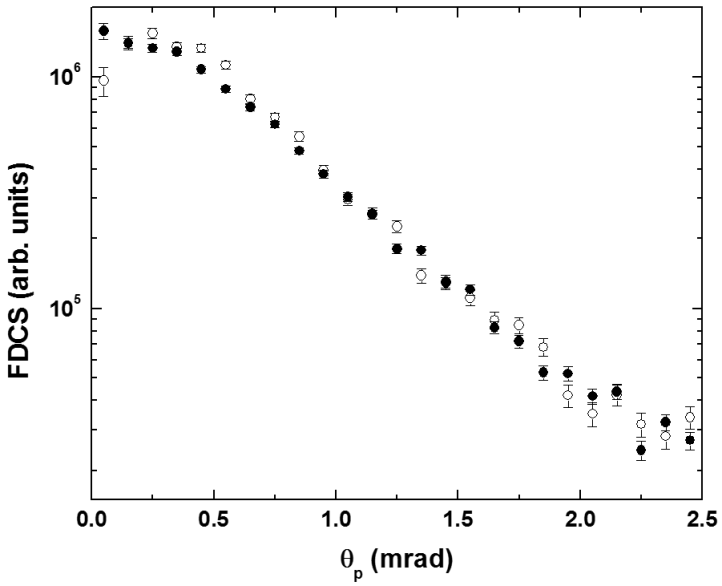

Figure 9. Same as Figure 5 for double capture, but integrated over all KER.

arly identifed in the data. A fit of I_2 (with and without π phase shift) to the coherent to incoherent FDCS ratios for the parallel orientation suggests an upper limit of the visibility factor α of 0.2. Furthermore, if any interference structure is present at all (i.e., if $\alpha > 0$) then the fit slightly favors the interference term without a phase shift.

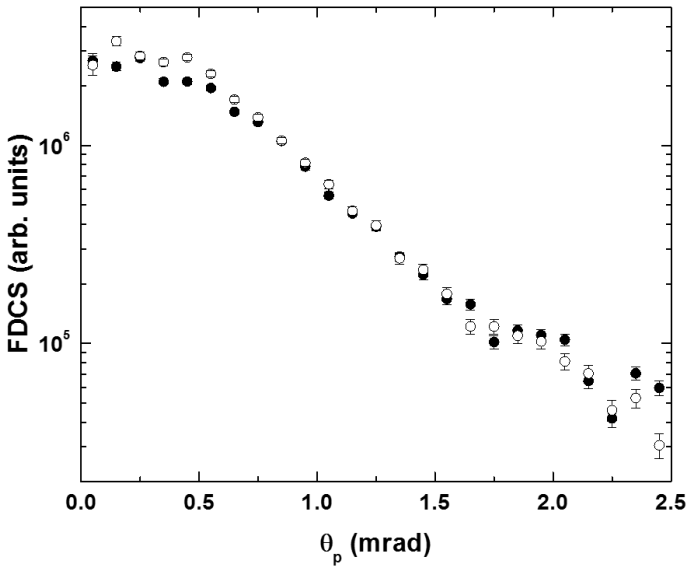

Figure 10. Same as Figure 6 for double capture, but integrated over all KER.

If the (near-) absence of two-center interference for the parallel orientation is primarily caused by the integration over all KER (i.e. by the spread in D) then one would expect that setting a condition on KER would lead to a visible interference pattern. For two reasons such a condition should have a more sensitive effect on the visibility than for dissociative single capture. First, since for double capture Coulomb explosion is the only fragmentation channel D is unambiguously determined by the KER value. Furthermore, since both electrons are removed from the molecule by the double capture process the relation between D and KER is not afflicted with any uncertainties introduced by screening.

Second, for double capture we achieved better statistics than for dissociative capture and as a result conditions on KER could be set with narrower windows.

In Figure 11 FDCS for the parallel orientation are shown for KER ranges of 13-18 eV (top panel), 18-22 eV (center panel), and 22-27 eV (bottom panel). Here, too, no substantial differences between the coherent and incoherent data are observed for any of the KER ranges. This suggests that the (near-) absence of interference structures is not primarily caused by any uncertainty in D. Rather, multiple scattering of the projectile from the target seems to be mostly responsible for a "washing out" of the interference pattern. In this case, a pronounced interference structure should be observable for much faster projectiles. In this regime double capture predominantly occurs through a correlated process, i.e. a single-scattering process. Indeed, pronounced interference structures were observed in double capture cross sections as a function of the molecular orientation in fast $He^{2+} + H_2$ collisions [36].

It seems plausible that the reduced visibility of the interference structure for dissociative capture, compared to vibrational dissociation, is mostly due to multiple scattering as well. Then, the three data sets on molecular fragmentation, for vibrational dissociation (published in Ref. [30]), for dissociation by an electronic transition to a repulsive state, and for double capture, exhibit a systematic trend: the visibility seems to be the smaller the more violent (on average) the collision between the projectile and the target. More specifically, the visibility maximizes for the one-electron process vibrational dissociation, presumably favoring relatively distant collisions, and minimizes for double capture, presumably the process which is most selective on close collisions.

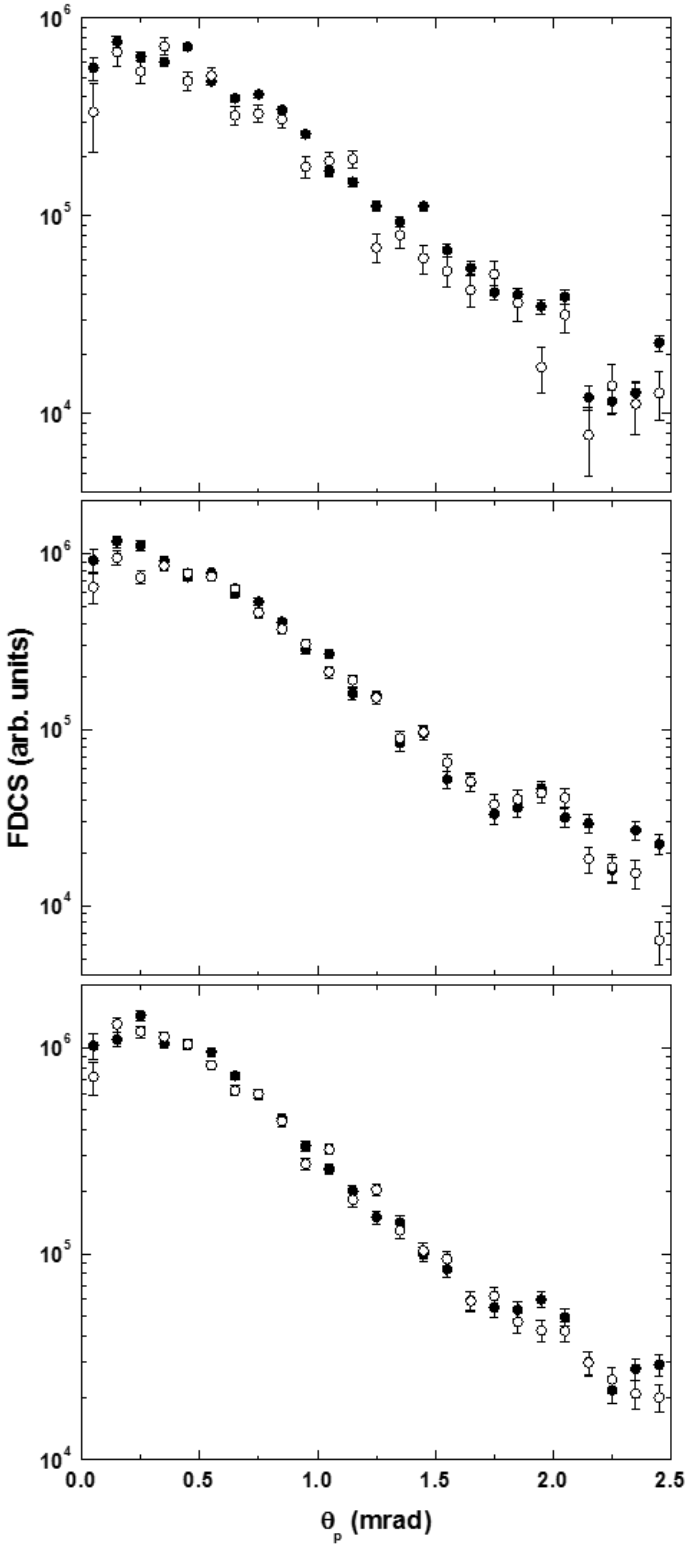

Figure 11. Same as Figure 10, but KER fixed at 13 to 18 eV (top panel), 18-22 eV (center panel), and 22-27 eV (bottom panel).

5. CONCLUSIONS

We have measured fully differential cross sections for dissociative single capture through excitation of the second electron to a repulsive state and for double capture leading to Coulomb explosion. Data were obtained for molecular orientations perpendicular and parallel to the transverse component of the momentum transfer, respectively. For neither process did we observe any signature of single-center interference effects, which are quite pronounced in the FDCS for vibrational dissociation for the perpendicular orientation [30]. Two-center interference structures were found in the FDCS for the parallel orientation for dissociative single capture. Here, contrary to vibrational dissociation, no phase shift of π in the interference term was found. Since the data are dominated by electron excitation to a gerade state this is consistent with the explanation that such a phase shift can occur if the symmetry of the electronic state switches [12,16].

For double capture at most only a very weak interference structure was found. Due to this very small (or zero) visibility for this process it is not possible to gain new insight from these data into the phase shift in the interference pattern that was observed in some cases, including our data on vibrational dissociation. So far, no systematic pattern has emerged that would suggest under what condition a phase shift may be present or not (apart from a switch in electronic symmetry). A phase shift has not been reported yet for processes in which the molecule does not fragment. However, for processes which do involve fragmentation, phase shifts were reported even when no switch in the symmetry of the electronic state occurred [15,30], or no phase shift was found although a switch in symmetry did occur [11]. Therefore, it seems important to study two-center interference in molecular fragmentation processes in more detail. So far, to the best of our knowledge,

a π phase shift was only clearly identified for fragmentation proceeding through a one-electron process [12,15,16,30]. Therefore, FDCS measurements for two-electron processes leading to fragmentation (like, e.g., double capture or double ionization) for fast projectiles would be particularly interesting. In this case two-electron processes are usually dominated by a correlated single scattering process and a pronounced interference structure should be observable. A confirmation of a pattern linking a phase shift to one-electron fragmentation processes by such measurements could represent a major step towards a complete understanding of the phase angle in the two-center interference term.

ACKNOWLEDGEMENTS

Support of this work by the National Science Foundation under Grants No. PHY-1401586 and No. PHY-1703109 is gratefully acknowledged.

REFERENCES

[1] H. Ehrhardt, K. Jung, G. Knoth, and P. Schlemmer, Z. Phys. D 1, 3 (1986)

[2] T. N. Rescigno, M. Baertschy, W. A. Issacs, and C. W. McCurdy, Science 286, 2474 (1999)

[3] M. Schulz, R. Moshammer, D. Fischer, H. Kollmus, D. H. Madison, S. Jones, and J. Ullrich, Nature 422, 48 (2003)

[4] M. Schulz, D. H. Madison, Int. J. Mod. Phys. A 21 3649 (2006)

[5] T. F. Tuan and E. Gerjuoy, Phys. Rev. 117, 756 (1960)

[6] S. Cheng, C. L. Cocke, V. Frohne, E. Y. Kamber, J. H. McGuire, and Y. Wang, Phys. Rev. A 47, 3923 (1993)

[7] N. Stolterfoht, B. Sulik, V. Hoffmann, B. Skogvall, J. Y. Chesnel, J. Ragnama, F. Frèmont, D. Hennecart, A. Cassimi, X. Husson, A. L. Landers, J. Tanis, M. E. Galassi, and R. D. Rivarola, Phys. Rev. Lett. 87, 23201 (2001).

[8] D. S. Milne-Brownlie, M. Foster, J. Gao, B. Lohmann, and D. H. Madison, Phys. Rev. Lett. 96, 233201 (2006)

[9] D. Misra, U. Kadhane, Y.P. Singh, L.C. Tribedi, P.D. Fainstein, and P. Richard Phys. Rev. Lett. 92, 153201 (2004)

[10] E.M. Staicu Casagrande, A. Naja, F. Mezdari, A. Lahmam-Bennani, P. Bolognesi, B. Joulakian, O. Chuluunbaatar, O. Al-Hagan, D. H. Madison, D.V. Fursa and I. Bray, J. Phys. B 41, 025204 (2008)

[11] H.T. Schmidt, D. Fischer, Z. Berenyi, C.L. Cocke, M. Gudmundsson, N. Haag, H.A.B. Johansson, A. Källberg, S.B. Levin, P. Reinhed, U. Sassenberg, R. Schuch, A. Simonsson, K. Stöchkel, and H. Cederquist, Phys. Rev. Lett. 101, 083201 (2008)

[12] L.Ph.H. Schmidt, S. Schössler, F. Afaneh, M. Schöffler, K.E. Stiebing, H. Schmidt-Böcking, and R. Dörner, Phys. Rev. Lett. 101, 173202 (2008)

[13] J.S. Alexander, A.C. Laforge, A. Hasan, Z.S. Machavariani, M.F. Ciappina, R.D. Rivarola, D.H. Madison, and M. Schulz, Phys. Rev. A 78, 060701(R) (2008)

[14] M.E. Galassi, R.D. Rivarola, and P.D. Fainstein, Phys. Rev. A 70, 032721 (2004)

[15] A. Senftleben, T. Pflüger, X. Ren, O. Al-Hagan, B. Najjari, D. Madison, A. Dorn, and J. Ullrich, J. Phys. B 43, 081002 (2010)

[16] S.F. Zhang, D. Fischer, M. Schulz, A.B. Voitkiv, J. Ullrich, X. Ma, and R. Moshammer, Phys. Rev. Lett. 112, 023201 (2014)

[17] K.N. Egodapitiya, S. Sharma, A. Hasan, A.C. Laforge, D.H. Madison, R. Moshammer, and M. Schulz, Phys. Rev. Lett. 106, 153202 (2011)

[18] S. Sharma, A. Hasan, K.N. Egodapitiya, T. P. Arthanayaka, and M. Schulz, Phys. Rev. A 86, 022706 (2012)

[19] S. Sharma, T.P. Arthanayaka, A. Hasan, B.R. Lamichhane, J. Remolina, A. Smith, and M. Schulz, Phys. Rev. A 90, 052710 (2014)

[20] T.P. Arthanayaka, S. Sharma, B.R. Lamichhane, A. Hasan, J. Remolina, S. Gurung, and M. Schulz, J. Phys. B 48, 071001 (2015)

[21] J.M. Feagin and L. Hargreaves, Phys. Rev. A 88, 032705 (2013)

[22] S. Sharma, T.P. Arthanayaka, A. Hasan, B.R. Lamichhane, J. Remolina, A. Smith, and M. Schulz, Phys. Rev. A 89, 052703 (2014)

[23] T.P. Arthanayaka, S. Sharma, B.R. Lamichhane, A. Hasan, J. Remolina, S. Gurung, L. Sarkadi, and M. Schulz, J. Phys. B 48, 175204 (2015)

[24] T. Arthanayaka, B.R. Lamichhane, A. Hasan, S. Gurung, J. Remolina, S. Borbély, F. Járai-Szabó, L. Nagy, and M. Schulz, J. Phys. B 49, 13LT02 (2016)

[25] M. Schulz in "Advances in Atomic, Molecular, and Optical Physics", Vol. 66, p. 508 edited by E. Arimondo, C.C. Lin, and S. Yelin, Elsevier, Cambridge MA, USA (2017)

[26] X. Wang, K. Schneider, A. LaForge, A. Kelkar, M. Grieser, R. Moshammer, J. Ullrich, M. Schulz, and D. Fischer, J. Phys. B45, 211001 (2012)

[27] K. Schneider, M. Schulz, X. Wang, A. Kelkar, M. Grieser, C. Krantz, J. Ullrich, R. Moshammer, and D. Fischer, Phys. Rev. Lett. 110, 113201 (2013)

[28] H. Gassert, O. Chuluunbaatar, M. Waitz, F. Trinter, H.-K. Kim, T. Bauer, A. Laucke, C. Müller, J. Voigtsberger, M. Weller, J. Rist, M. Pitzer, S. Zeller, T. Jahnke, L.Ph.H. Schmidt, J.B. Williams, S.A. Zaytsev, A.A. Bulychev, K.A. Kouzakov, H. Schmidt-Böcking, R. Dörner, Yu.V. Popov, and M.S. Schöffler, Phys. Rev. Lett. 116, 073201 (2016)

[29] F. Navarrete, M.F. Ciappina, L. Sarkadi, R.O. Barrachina, Nucl. Instrum. Meth. B, 408,165 (2017)

[30] B.R. Lamichhane, T. Arthanayaka, J. Remolina, A. Hasan, M.F. Ciappina, F. Navarrete, R.O. Barrachina, R.A. Lomsadze, and M. Schulz, Phys. Rev. Lett. 119, 083402 (2017)

[31] H.F. Busnengo, S.E. Corchs, and R.D. Rivarola, Phys. Rev. A 56, 1042 (1997)

[32] M. Dürr, B. Najjari, M. Schulz, A. Dorn, R. Moshammer, A.B. Voitkiv, and J. Ullrich, Phys. Rev. A75, 062708 (2007)

[33] I. Ben-Itzhak, V. Krishnamurthi, K.D. Carnes, H. Aliabadi, H. Knudsen, U. Mikkelsen, and B.D. Esry, J. Phys. B 29, L21 (1996)

[34] A. K. Edwards, R. M. Wood, J. L. Davis, and R. L. Ezell, Phys. Rev. A 42, 1367 (1990)

[35] A.K. Edwards and Q. Zheng, J. Phys. B 33, 881 (2000)

[36] D. Misra, H.T. Schmidt, M. Gudmundsson, D. Fischer, N. Haag, H.A.B. Johansson, A. Källberg, B. Najjari, P. Reinhed, R. Schuch, M. Schöffler, A. Simonsson, A.B. Voitkiv, and H. Cederquist, Phys. Rev. Lett. 102, 153201 (2009)

SECTION

2. CONCLUSIONS

An important role of interference and coherence effects in atomic fragmentation processes induced by ion impact, was recently uncovered in a series of experiments [31,38,39,40,41,46,47]. These studies strongly suggested that cross sections could be significantly affected by the projectile coherence properties, especially for fast and heavy ions because of their very small de Broglie wavelength. These findings were also supported by several theoretical investigations [42-44]. Since then our understanding of atomic collision dynamics, in general, evolved extensively. Thus, the projectile coherence property, which was unnoticed for decades, can now be regarded as being established.

The motivation for the experiments described in this dissertation was not primarily to provide further evidence for the importance of coherence properties, but rather to use it as a tool to study the few-body dynamics in detail. To this end, we have performed kinematically complete experiments for fragmentation of H_2 by 75keV proton impact. A new approach was used to analyze coherence and interference effects observable in the cross sections in detail. We used two narrow slits to collimate the projectile beam in the horizontal and vertical directions. The two slits were placed at different distances from the target such that the width of the projectile wave packet was either larger (coherent) or smaller (incoherent) compared to the target dimension in the y- and x- directions respectively. The idea was to measure cross sections for coherent and incoherent projectiles simultaneously under otherwise identical experimental conditions. That way, experimental artifacts, like, e.g., resolution effects, could be ruled out right from the onset as an

explanation for any differences between the cross sections measured for coherent and incoherent projectiles.

In the first journal article of my dissertation, fully differential cross sections for single electron capture accompanied by vibrational dissociation was measured. This is a single electron process, for which the second electron stays in the electronic ground state and excitation of the nuclear motion to a vibrational continuum state triggers dissociation of the molecule. Cross-sections were analyzed for a fixed kinetic energy release (KER) of 0 – 2eV in the dissociation and for two different molecular orientations (referred to as perpendicular and parallel orientations in the journal Paper I) as a function of projectile scattering angle. Differences between coherent and incoherent FDCS were observed for both the perpendicular and parallel molecular orientations. In the coherent to incoherent cross-sectional ratios, which represents the interference term, we observed pronounced structures due to single-center interference for the perpendicular orientation and a combination of single- and two-center interference for the parallel orientation. Two-center interference could be extracted by dividing the ratios for the parallel orientation by the single-center interference term. An unexpected phase shift of π in the phase angle was seen in the pronounced oscillations of the two-center interference term. The 2-center interference pattern was very well reproduced by the theoretical interference term of equation (3) of the introduction, but only if a π phase shift was included. However, its origin is not currently understood.

Schmidt et al. [30] observed a similar double slit interference pattern in measured dissociative electron transfer cross-sections from He into 10keV H_2^+ ions. A dissociation pathway was selected for which the active electron is captured from the symmetric ground

state of the He atom to the $2p\sigma_u$ state, i.e., an anti-symmetric orbital state of the molecule. The observed interchanging of interference minima and maxima, when compared to optical double slit interference, was explained as due to the switch in the symmetry of the electronic state. This explanation is basically an application of parity conservation. To conserve the total parity of the system, the projectile must switch its symmetry to compensate the switch in the symmetry of the electronic state, and this should lead to a π phase shift in the interference term. The same phase shift was also reported for dissociative excitation [36] and explained by the same symmetry arguments given in Ref. [30].

However, no phase shift was found in collisions of protons capturing one electron from H_2 molecules accompanied by excitation of the second electron on the molecule to repulsive $2p\sigma_u$ state (transfer excitation, TE) [48,49]; although, here too a switch of symmetry in the electronic state occurs. Thus, a phase shift of π would be expected based on the symmetry arguments described earlier [30]. Later, in an experiment studying dissociative ionization due to electron impact [50], a phase shift in the interference pattern was observed. This is remarkable because no change of symmetry in the electronic state occurred. This experimental observation was also reproduced by a theoretical calculation, where the interference term was included from first principles. The three data sets of Refs. [48,50] and the data presented in the first journal article of this dissertation for the case of vibrational dissociation showed opposite behavior to the expectation based on the symmetry of the electronic state. Hence, there must be some other factors apart from the electronic symmetry that can either lead to or counteracts a phase shift in the interference term. This indicates that the phase angle in the interference term is not fully understood yet.

In the second journal article of this dissertation, we reported measured FDCS for two other molecular fragmentation channels. In one, single capture accompanied by excitation of the second electron, i.e., transfer excitation leading to a repulsive state was investigated. In the second, double electron capture leading to Coulomb explosion was studied. The motivation to investigate these processes was to study the phase shift observed in the first project more systematically. Data for TE were analyzed for KER values corresponding to dissociation proceeding through the $2s\sigma_g$ (gerade symmetry) and the $2p\pi_u$ (ungerade symmetry) states. No clear signature of single-center interference effects was seen. Thus, unlike the earlier case of vibrational dissociation, we mainly focused on the parallel molecular orientation, in which two-center interference structures were found. However, no phase shift of π was observed in the interference term, differing from the earlier observation in the case of vibrational dissociation. This is consistent with the symmetry arguments stated in Ref. [30] as the data are dominated by the excitation of electrons to the gerade (i.e., symmetric) orbital state for large scattering angle (θ_p). On the other hand, for smaller θ_p, we have only a few data points with relatively large statistical fluctuations so that no conclusions can be made.

For the other fragmentation channel, i.e., Coulomb explosion induced by double capture, we observed at most only a very weak interference structure for both molecular orientation. As far as a phase shift in the interference pattern is concerned, no new insight was obtained. So far, no systematic pattern has appeared that would suggest under what context a phase shift may be present or absent. A phase shift in the interference term has only been reported for processes, which involves fragmentation of molecules. However, such a shift was found for cases with and without a switch in the symmetry of electronic

state [48-50]. On the other hand, a phase shift in the interference pattern has not been reported yet for processes in which the molecule does not fragment. Furthermore, a π phase shift was only clearly identified for fragmentation through a single-electron process. Thus, it is particularly interesting to investigate two-center interference, in fragmentation processes proceeding through the two-electron process (like, e.g., double capture or double ionization) at large projectile velocity. The advantage is that for fast projectiles a correlated single scattering process usually dominates the two-electron process and a pronounced interference structure should be observed. This will be a major step towards gaining new insights of the phase angle in the two-center interference term, and consequently to further our understanding of few-body dynamics.

In this dissertation, taking advantage of our knowledge about projectile coherence effects, two distinct types of interference, namely single- and two-center interference was studied. Some unexpected observations were made in two-center interference, which we expect to initiate significant further research activities in this area.

BIBLIOGRAPHY

[1] C. Froese-Fischer, T. Brage, and P. Johnsson, Computational Atomic Structure: An MCHF Approach, CRC Press (1997)

[2] M. Schulz, R. Moshammer, D. Fischer, H. Kollmus, D. H. Madison, S. Jones, and J. Ullrich, Nature(London) 422, 48 (2003).

[3] M. Schulz and D. H. Madison, Int. J. Mod. Phys. A 21, 3649 (2006).

[4] T.N. Rescigno, M. Baertschy, W.A. Isaacs, and C.W. McCurdy, Science 286, 2474 (1999).

[5] M. Dürr, C. Dimopoulou, A. Dorn, B. Najjari, I. Bray, D. V. Fursa, Z. Chen, D. H. Madison, K. Barschat, and J. Ullrich, Journal of Physics B. 39, 4097 (2006)

[6] M. Dürr, C. Dimopoulou, A. Dorn, B. Najjari, K. Barschat, I. Bray, D. V. Fursa, Z. Chen, D. H. Madison, and J. Ullrich, Phys. Rev. A 77, 032717 (2008)

[7] X. Ren, A. Senftleben, T. Pflüger, A. Dorn, J. Colgan, M.S. Pindzola, O. Al-Hagan, D. H. Madison, I. Bray, D. V. Fursa, and J. Ullrich, Phys. Rev. A, 82, 032712 (2010)

[8] R. Dörner, V. Mergel, R. Ali, U. Buck, C.L. Cocke, K. Froschauer, O. Jagutzki, S. Lencinas, W.E. Meyerhof, S. Nüttgens, R. E. Olson, H. Schmidt-Böcking, L. Spielberger, K. Tökesi, J. Ullrich, M. Unverzagt, and W. Wu, Phys. Rev. Lett. 72, 3166 (1994).

[9] J. Ullrich, R. Moshammer, R Dörner, O. Jagutzki, V. Mergel, H. Schmidt-Böcking and L. Spielberger, J. Phys. B 30, 2917 (1997).

[10] R. Moshammer, M. Unverzagt, W. Schmitt, J. Ullrich, and H. Schmidt-Böcking, Nucl. Instrum. Methods Phys. Res. B 108, 425 (1996).

[11] J. Ullrich, R. Moshammer, R. Dörner, O. Jagutzki, V. Mergel, H. Schmidt-Böcking and L. Spielberger, Rep. Prog. Phys. 66 1463 (2003).

[12] H. Ehrhardt, K. Jung, G. Knoth, and P. Schlemmer, Z. Phys. D, Z. Phys. D 1, 3 (1986).

[13] I. Bray, J. Phys. B 33, 581 (2000).

[14] J. Colgan, M. S. Pindzola, Phys. Rev. A 74, 012713 (2006).

[15] M. F. Ciappina, W. R. Cravero, M. Schulz, R. Moshammer, and J. Ullrich, Phys. Rev. A 74, 042702 (2006).

[16] A. B. Voitkiv and B. Najjari, Phys. Rev. A 79, 022709 (2009).

[17] D. H. Madison, D. Fischer, M. Foster, M. Schulz, R. Moshammer, S. Jones, and J. Ullrich, Phys. Rev. Lett. 91, 253201 (2003).

[18] H. Ehrhardt, M. Schulz, T. Tekaat, and K. Willmann, Phys. Rev. Lett. 22, 89 (1969).

[19] M. Schulz, M. F. Ciappina, T. Kirchner, D. Fischer, R. Moshammer, and J. Ullrich, Phys. Rev. A 79, 042708 (2009).

[20] M. Schulz, Phys. Scr. 80, 068101 (2009).

[21] D. Madison, M. Schulz, S. Jones, M. Foster, R. Moshammer and J. Ullrich, J. Phys. B 35 3297 (2002).

[22] M. Schulz, M. Dürr, B. Najjari, R. Moshammer, and J. Ullrich, Phys. Rev. A 76, 032712 (2007).

[23] I. B. Abdurakhmanov, I. Bray, D. V. Fursa, A. S. Kadyrov, and A. T. Stelbovics, Phys. Rev. A, 86, 034701 (2012).

[24] M. S. Pindzola and F. Robicheaux, Phys. Rev. A, 82, 042719 (2010).

[25] S. Cheng, C. L. Cocke, V. Frohne, E. Y. Kamber, J. H. McGuire, andY. Wang, Phys. Rev. A 47, 3923 (1993)

[26] N. Stolterfoht, B. Sulik, V. Hoffmann, B. Skogvall, J. Y. Chesnel, .1. Ragnama, F. Fremont D. HennecarL A. Cassimi, X. Husson, A. L. Landers. J. Tanis, M. E. Galassi. and R. D. Rivarola, Phys. Rev. Lett. 87, 23201 (2001).

[27] N. Stolterfoht et al., Phys. Rev. A 67, 030702 (2003)

[28] D. Misra, U. Kadhane, Y. P. Singh, L. C. Tribedi, P. D. Fainstein, and P. Richard, Phys. Rev. Lett.92, 153201 (2004)

[29] D. Misra, H. T. Schmidt, M. Gudmundsson, D. Fischer, N. Haag, H.A.B. Johansson, A. Kallberg, B. Najjari, P. Rcinhcd, R. Schuch, M. Schoft1er, A. Simonsson, A.B. Voitkiv, and H. Cederquist, Phys. Rev. Lett. 102, 153201 (2009)

[30] L. Ph. H. Schmidt, S. Schosslcr, F. Afaneh, M. Schoffler, K. E. Stiebing, H. Schmidt-Backing, and R. Dorner, Phys. Rev. Lett. 101, 173202 (2008)

[31] K. N. Egodapitiya, S. Sharma, A. Hasan, A. C. Laforge, D. H. Madison, R. Moshammer, and M. Schulz, Phys. Rev. Lett. 106, 153202 (2011)

[32] T. F. Tuan and E. Ge1juoy, Phys. Rev. 117, 756 (1960)

[33] H. D. Cohen and U. Fano, Phys. Rev. 150 (1966)

[34] J.S. Alexander, A.C. Laforge, A. Hasan, Z.S. Machavariani, M.F. Ciappina, R.D. Rivarola, D.H. Madison, and M. Schulz, Phys. Rev. A 78, 060701(R) (2008)

[35] A. Messiah, Quantum Mechanics Vol.2

[36] S.F. Zhang, D. Fischer, M. Schulz, A.B. Voitkiv, J. Ullrich, X. Ma, and R. Moshammer, Phys. Rev. Lett. 112, 023201 (2014)

[37] J.M. Feagin and L. Hargreaves, Phys. Rev. A, 88, 032705 (2013).

[38] S. Sharma, T.P. Arthanayaka, A. Hasan, B.R. Lamichhane, J. Remolina, A. Smith, and M. Schulz, Phys. Rev., A 89, 052703 (2014)

[39] S. Sharma, T.P. Arthanayaka, A. Hasan, B.R. Lamichhane, J. Remolina, A. Smith, and M. Schulz, Phys. Rev. A 90, 052710 (2014)

[40] T.P. Arthanayaka, S. Sharma, B.R. Lamichhane, A. Hasan, J. Remolina, S. Gurung, and M. Schulz, J. Phys. B 48, 071001 (2015)

[41] T. Arthanayaka, B.R. Lamichhane, A. Hasan, S. Gurung, J. Remolina, S. Borbély, F. Járai-Szabó, L. Nagy, and M. Schulz, J. Phys. B 49, 13LT02 (2016)

[42] L. Sarkadi, I. Fabre, F. Navarrete, and R. Barrachina, Phys. Rev. A 93, 032702 (2016)

[43] F. Navarrete, M.F. Ciappina, L. Sarkadi, and R.O. Barrachina, Nucl. Instrum. Meth. B, 408, 165 (2017)

[44] A. Igarashi and L. Gulyas, J. Phys. B 50, 035201 (2017)

[45] Borbély S, Feist J, Tőkési K, Nagele S, Nagy L and Burgdörfer J 2014 Phys. Rev. A 90 052706

[46] S. Sharma, A. Hasan, K.N. Egodapitiya, T. P. Arthanayaka, and M. Schulz, Phys. Rev. A 86, 022706 (2012)

[47] T.P. Arthanayaka, S. Sharma, B.R. Lamichhane, A. Hasan, J. Remolina, S. Gurung, L. Sarkadi, and M. Schulz, J. Phys. B, 48, 175204 (2015)

[48] H. T. Schmidt, D. Fischer, Z. Berenyi, C. L. Cocke, M. Gudmundsson, N. Haag, H. A. B. Johansson, A. Ka¨llberg, S. B. Levin, P. Reinhed, U. Sassenberg, R. Schuch, A. Simonsson, K. Støchkel, and H. Cederquist, Phys. Rev. Lett. 101, 083201 (2008).

[49] K. Støchkel, O. Eidem, H. Cederquist, H. Zettergren, P. Reinhed, R. Schuch, C. L. Cocke S. B. Levin, V. N. Ostrovsky, A. Kälberg, A. Simonsson, J. Jensen, and H. T. Schmidt, Phys. Rev. A 72, 050703 (2005).

[50] A. Senftleben, T. Pflüger, X. Ren, O. Al-Hagan, B. Najjari, D. Madison, A. Dorn, and J. Ullrich, J. Phys. B 43, 081002 (2010).

VITA

Basu Ram Lamichhane was born in Nuwakot, Nepal. He received a Bachelor of Science degree from Tribhuvan University, Amrit Science Campus, Kathmandu, Nepal in March 2008. He received a Master of Science in Physics from Tribhuvan University, Patan Multiple Campus, Lalitpur, Nepal in November 2010. In Fall 2012, he joined the Department of Physics at Missouri University of Science and Technology (Missouri S&T), Rolla, USA where he received an MS in Physics (Summer 2015). Here, he worked as a Graduate Teaching Assistant and Graduate Research Assistant from Fall 2013 till Spring 2018. He received his Ph.D. degree in Physics from Missouri S&T in May 2018, for his work on "Fully Differential Study of Vibrational Dissociation in $p + H_2$ Collisions". He performed his research at the Laboratory of Atomic, Molecular and Optical Research(LAMOR) in a group under the guidance of Professor Dr. Michael Schulz.

While at Missouri S&T, Basu had contributed to the publication of nine journal papers, including a first-author article in Physical Review Letters. He had presented his research work at 70th Annual Gaseous Electronic Conference in November 2017, where he was selected as a finalist for Student Excellence Award. In December 2017, he was awarded the 1st prize in 24th Annual Schearer Prize for Research by the Department of Physics, Missouri S&T.

He volunteered for the Council of Graduate Students at Missouri S&T; as the Physics Department representative from August 2013 till May 2014, and as a Treasurer from May 2014 until May 2015. As an executive member of the Council of Graduate Students, Missouri S&T honored him by the Chancellor's Challenge Award in May 2015 for his service.